The HI intensity mapping power spectrum

insights from recent measurements

Hamsa Padmanabhan
Scientific collaborator and PI, SNSF Ambizione Grant
Université de Genève

Based on:
Hamsa Padmanabhan, Roy Maartens, Obinna Umeh and Stefano Camera (2023), *under review,* arXiv:2305.09720
Hamsa Padmanabhan (2023), MNRAS 523 (3), 3503, arXiv:2212.08077

Intensity mapping in the post-reionization Universe

Intensity mapping (IM)

[Early studies: Hogan and Rees 1979, Sunyaev and Zeldovich 1972,1974, Bebington+ 1986]

- Measure all structure; sensitive to the integrated emission of all the sources; including foregrounds
- Foregrounds are spectrally smooth, different from the signal
- Different environments, different lines

Credit: Dongwoo Chung

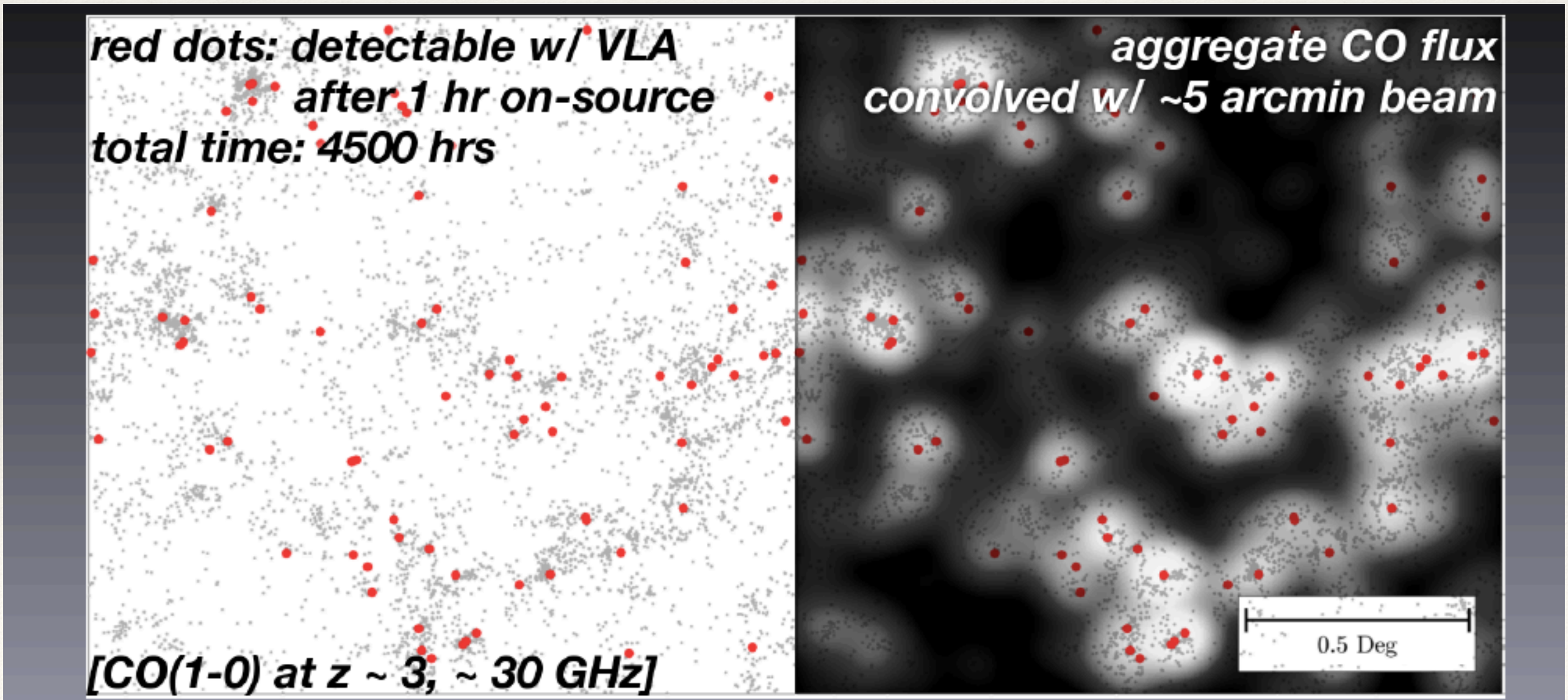

The power spectrum

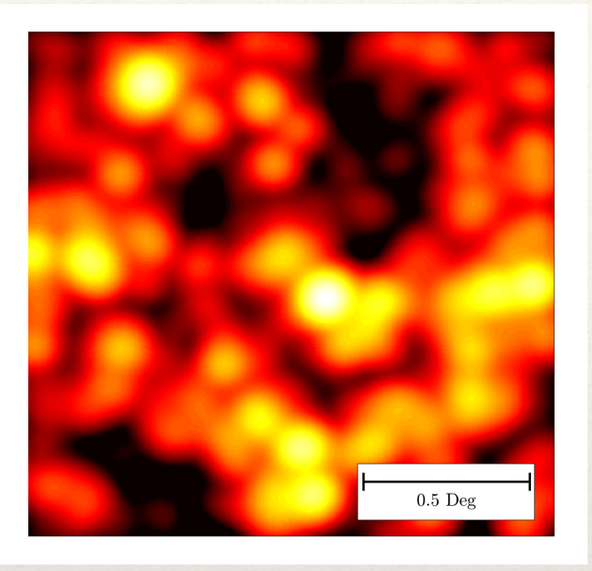

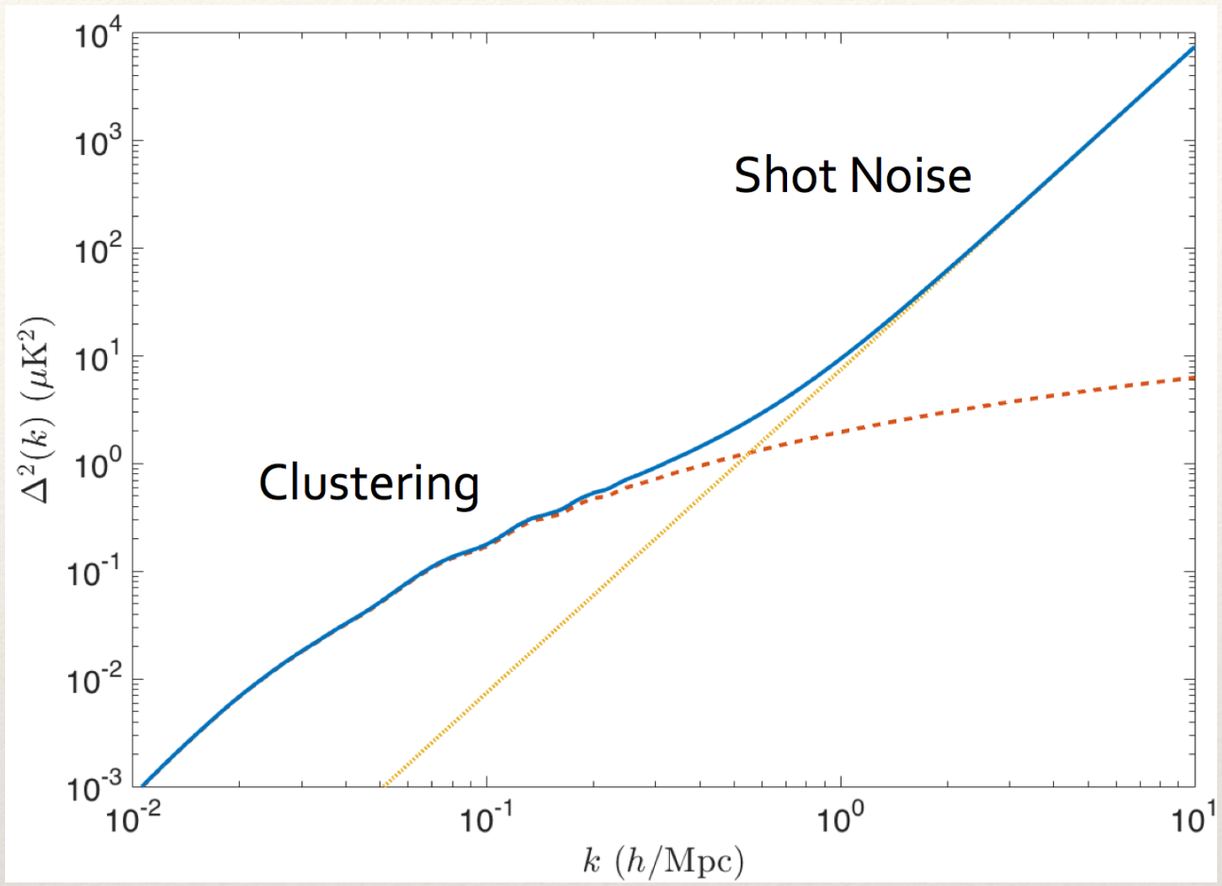

$$P_{\rm line}(k,z) = \langle I(z)\rangle^2 b^2(z) P_{\rm cdm}(k,z) + P_{\rm shot}(z)$$

Abundance **Bias** **Shot noise**

Clustering

The ‘astrophysical systematic’

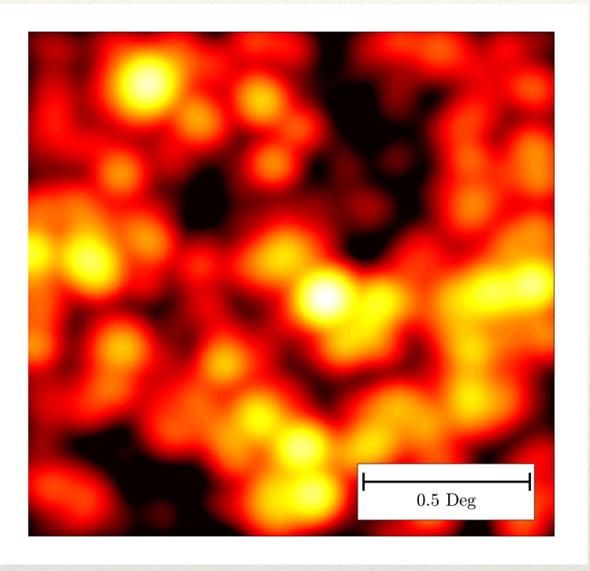

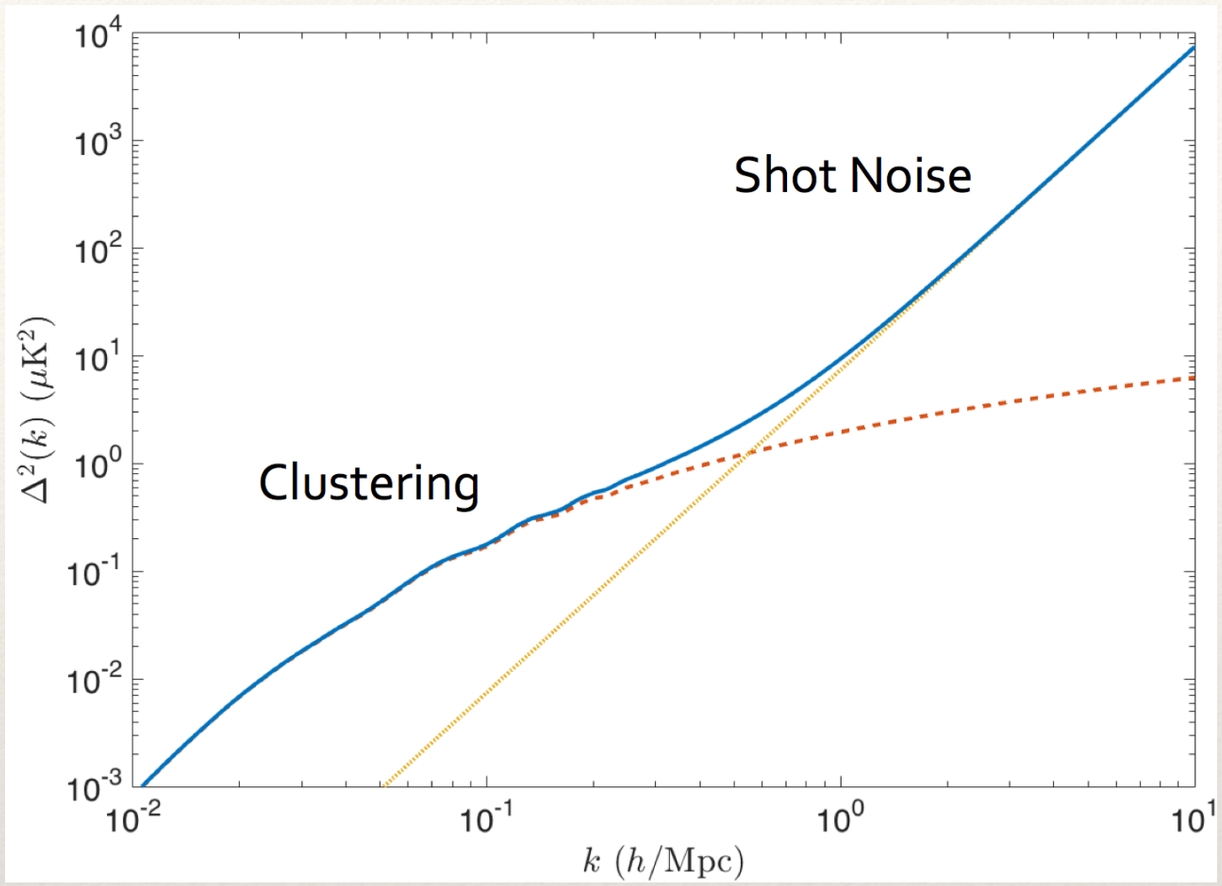

$$P_{\rm line}(k,z) = \langle I(z)\rangle^2 b^2(z) P_{\rm cdm}(k,z) + P_{\rm shot}(z)$$

ASTROPHYSICS **COSMOLOGY**

There is an interplay of astrophysics and cosmology

How can we quantify this in predictions?

Model the astrophysics efficiently …

… using a halo model for baryonic gas

[Seljak (2000), White (2000), Cooray and Sheth (2002) …. Asgari et al. (2023)]

***Hamsa Padmanabhan**, Alexandre Refregier, Adam Amara,*
MNRAS 469 (2), 2323 (2017) [arXiv:1611.06235]

***Hamsa Padmanabhan**, Alexandre Refregier, MNRAS 464(4), 4008 (2017)*
[arXiv:1607.01021]

***Hamsa Padmanabhan**, Alexandre Refregier, Adam Amara,*
MNRAS 485 (3), 4060 (2019) [arXiv:1804.10627]

***Hamsa Padmanabhan**, Alexandre Refregier, Adam Amara,*
MNRAS 495 (4), 3935 (2020) [arXiv:1909.11104]

The tracer-halo connection

$$P_{\rm line}(k,z) = \underbrace{\langle I(z)\rangle^2 b^2(z) P_{\rm cdm}(k,z)}_{\text{Bias times line intensity}} + \underbrace{P_{\rm shot}(z)}_{\text{Matter fluctuations}}$$

$$b(z) \propto \int dM_h \frac{dn}{dM_h}(z)\ \underbrace{L_{\rm tr}(M_h,z)}_{\text{Tracer-halo relation}}\ \overbrace{b_h(M_h)}^{\text{Halo bias}}$$

$$I(z) \propto \int \underbrace{dM_h \frac{dn}{dM_h}(z)}_{\text{Halo mass function}}\ L_{\rm tr}(M_h,z)$$

$$P_{\rm 1h} \propto \underbrace{\int dM_h\ \frac{dn}{dM_h}\ L_{\rm tr}(M_h,z)^2}_{\text{Shot noise}}\ \underbrace{|u_{\rm tr}(k|M)|^2}_{\text{Small scales; tracer profile in halo}}$$

A halo model for neutral hydrogen

Combine IM observations with individual objects

$M_{\rm HI}\ (M_h, z)$

Average HI mass

associated with

a halo of mass M

at redshift z

$\rho_{\rm HI}\ (r; M_h, z)$

Radial HI distribution

within

a halo of mass M

at redshift z

Allows us to derive HI observables

[HP, Choudhury, Refregier, MNRAS (2016)]

[Barnes & Haehnelt (2010, 2014), Villaescusa-Navarro + (2015), …]

$$M_{\rm HI}(M,z) = \alpha f_{\rm H,c} M \left(\frac{M}{10^{11} h^{-1} M_\odot}\right)^{\beta} \exp\left[-\left(\frac{v_{c,0}}{v_c(M,z)}\right)^3\right]$$

HI Fraction relative to cosmic — **Slope** — **Lower cutoff**

HI HALO MODEL

$$\rho_{\rm HI}(r,M,z) \quad \rho_0 \exp(-r/r_s);\ r_s = R_v(M)/c_{\rm HI}(M,z)$$

$$c_{\rm HI}(M,z) = c_{\rm HI,0} \left(\frac{M}{10^{11} M_\odot}\right)^{-0.109} \frac{4}{(1+z)^{\gamma}}$$

concentration parameter — **Evolution with redshift**

[e.g. Wang+ (2014), Bigiel & Blitz (2012)…]

A halo model for HI

[HP+, MNRAS (2017a, b), HP & Kulkarni (2017)]

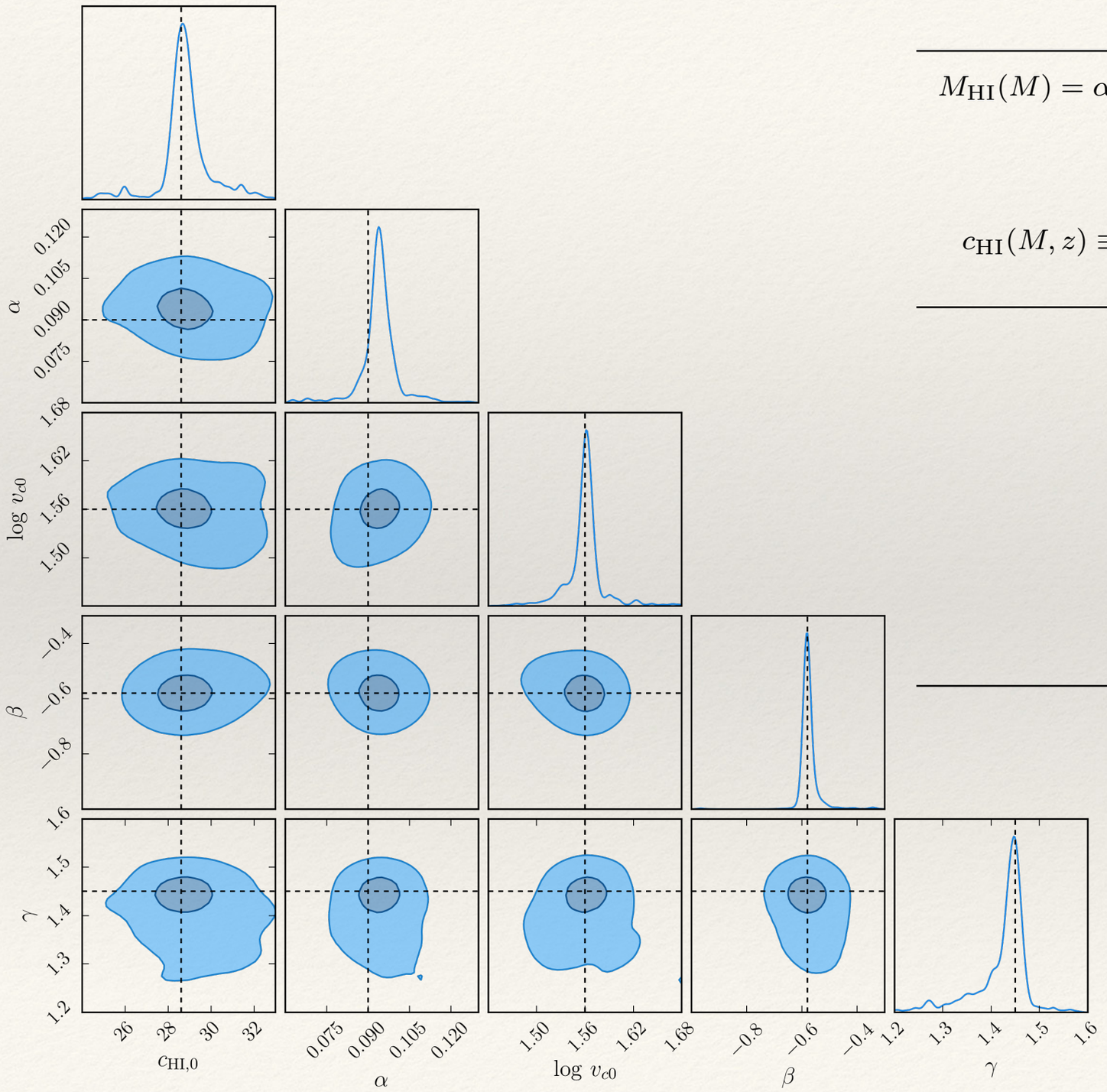

$$M_{\rm HI}(M) = \alpha f_{H,c} M \left(M/10^{11} h^{-1} M_\odot\right)^{\beta} \exp\left[-\left(v_{c0}/v_c(M)\right)^3\right]$$

$$\rho_{\rm HI}(r) = \rho_0 \exp(-r/r_s);$$

$$c_{\rm HI}(M,z) \equiv R_v/r_s = c_{\rm HI,0}\left(M/10^{11} M_\odot\right)^{-0.109} 4/(1+z)^{\gamma}$$

$$c_{\rm HI,0} = 28.65 \pm 1.76$$

$$\alpha = 0.09 \pm 0.01$$

$$\log v_{c,0} = 1.56 \pm 0.04$$

$$\beta = -0.58 \pm 0.06$$

$$\gamma = 1.45 \pm 0.04$$

CONSTRAINTS FROM CURRENT HI GALAXY, DLA, IM DATA

One shoe fits all!

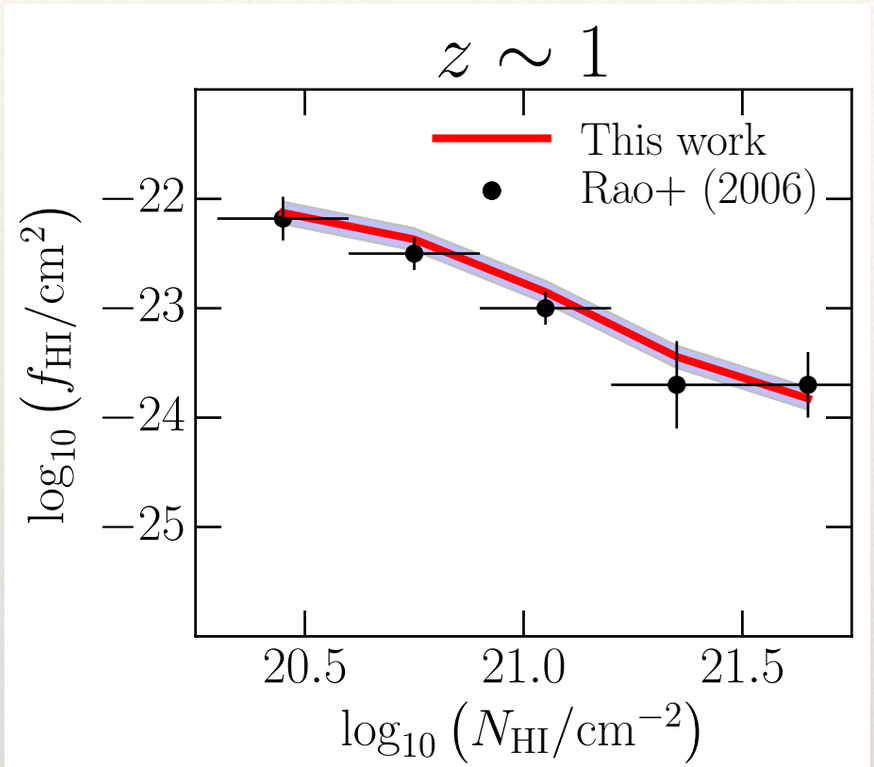

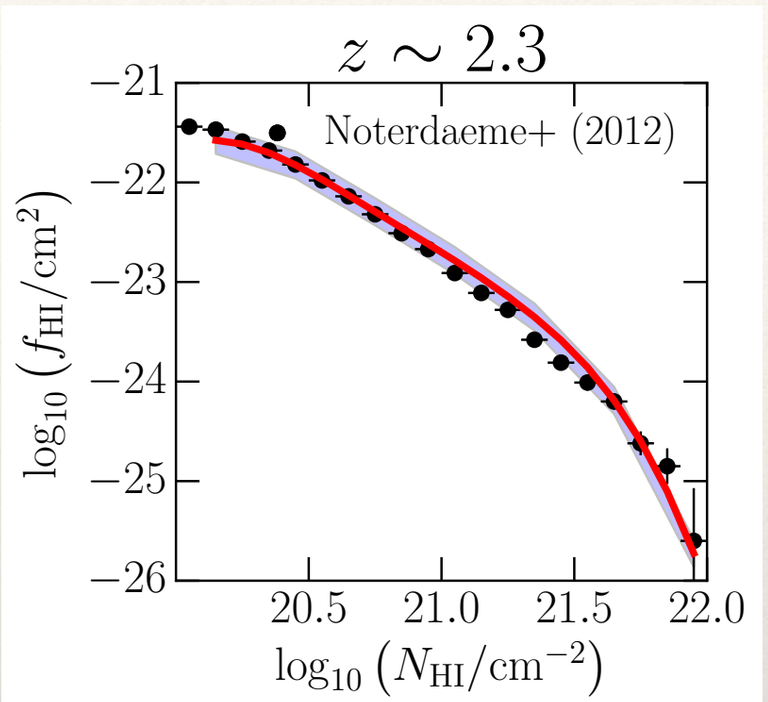

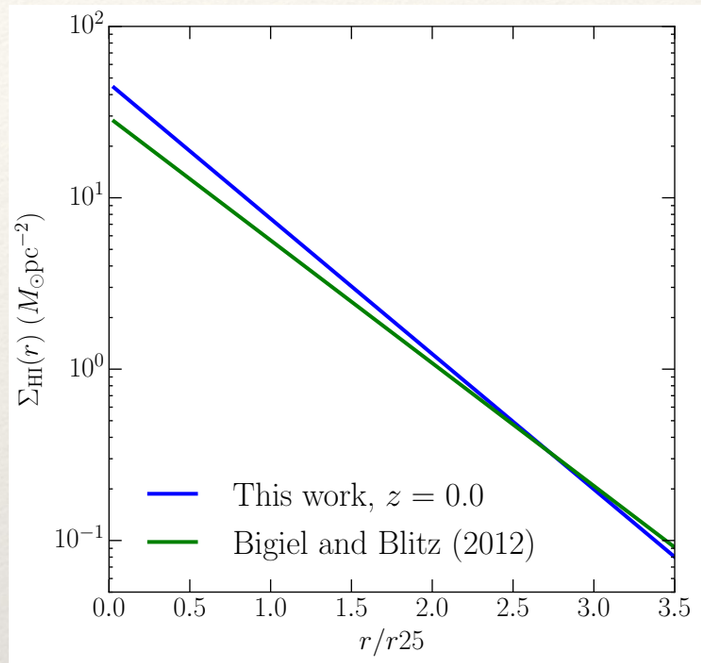

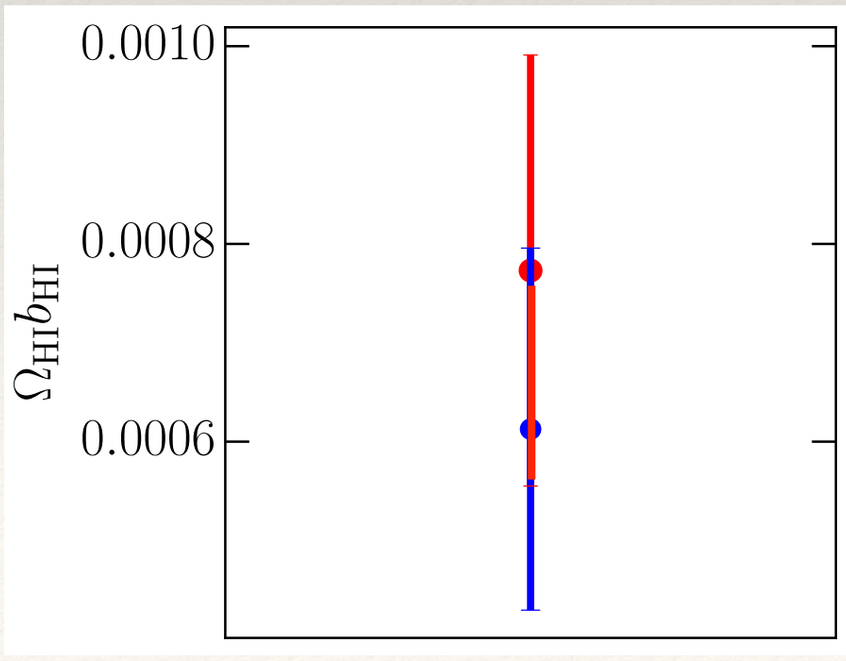

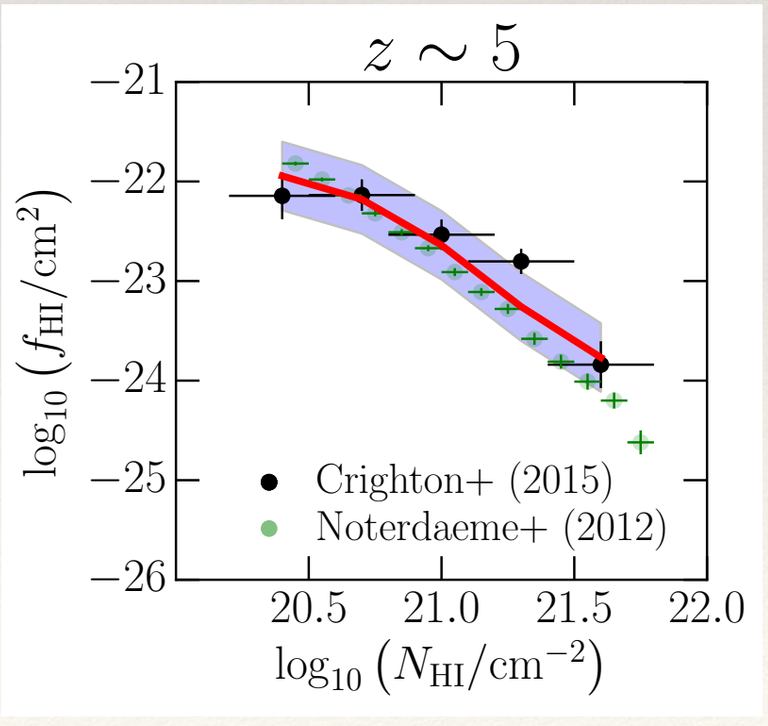

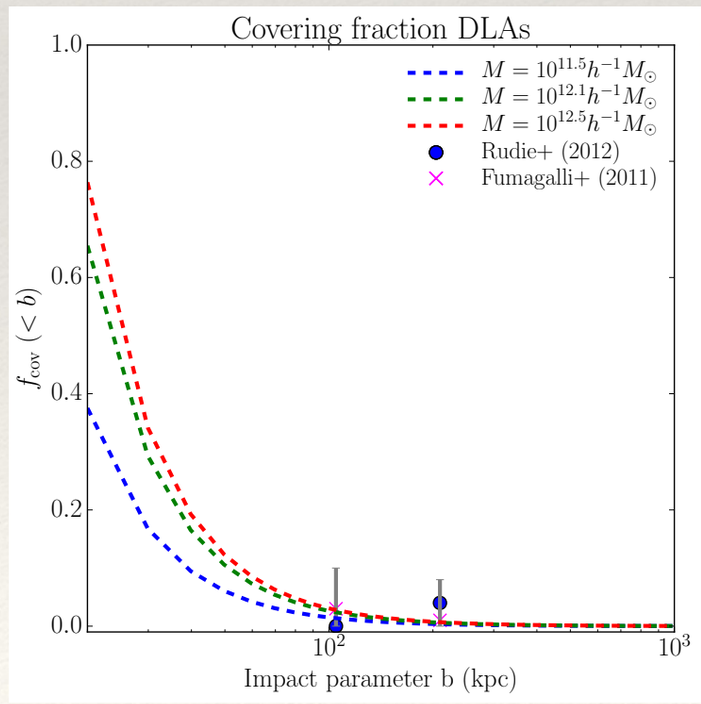

Best fit halo model

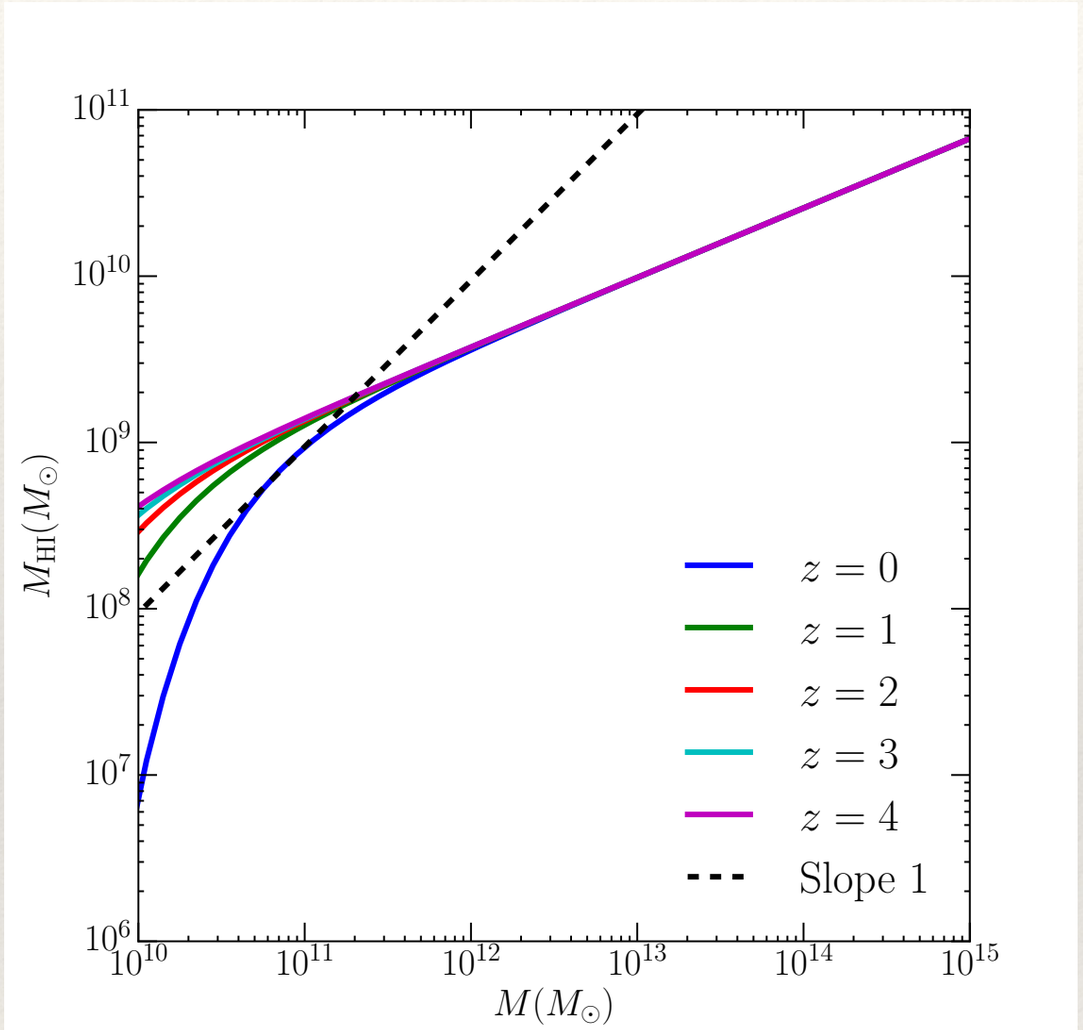

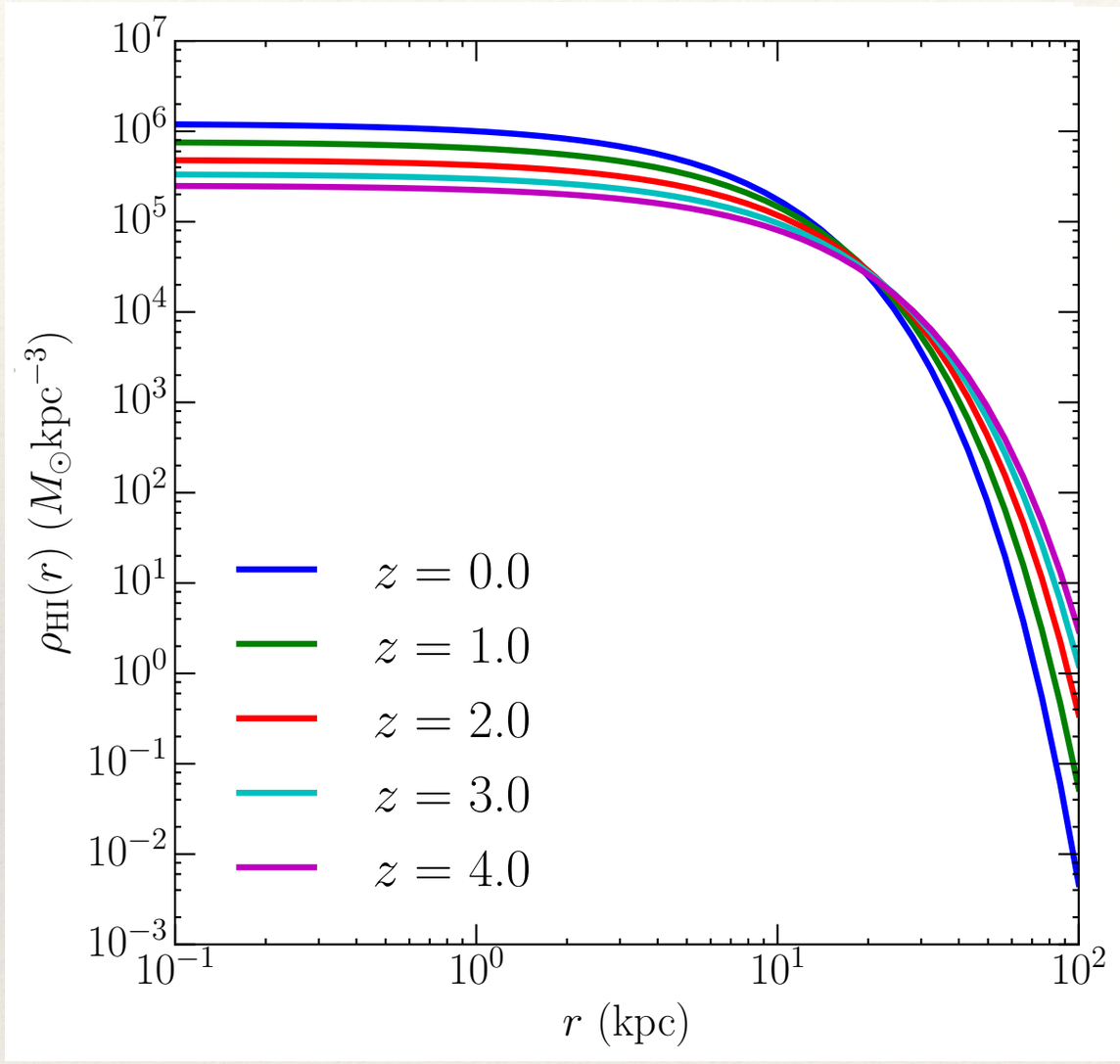

[HP, Refregier, Amara, MNRAS (2017)]

Non-unity slope!

Exponential profile

Interpreting the latest results : extensions to redshift space

***Hamsa Padmanabhan**, Roy Maartens, Obinna Umeh, Stefano Camera (2023), The HI intensity mapping power spectrum: insights from recent observations, submitted, [arXiv:2305.09720]*

SKAO Pathfinder: MeerKAT

- 64 dishes
- Will become part of SKA-MID
- $0.2 < z < 0.58$ (L-band)
- $0.4 < z < 1.45$ (UHF-band)
- ~4000 sq.deg surveys

credit: Steve Cunnington

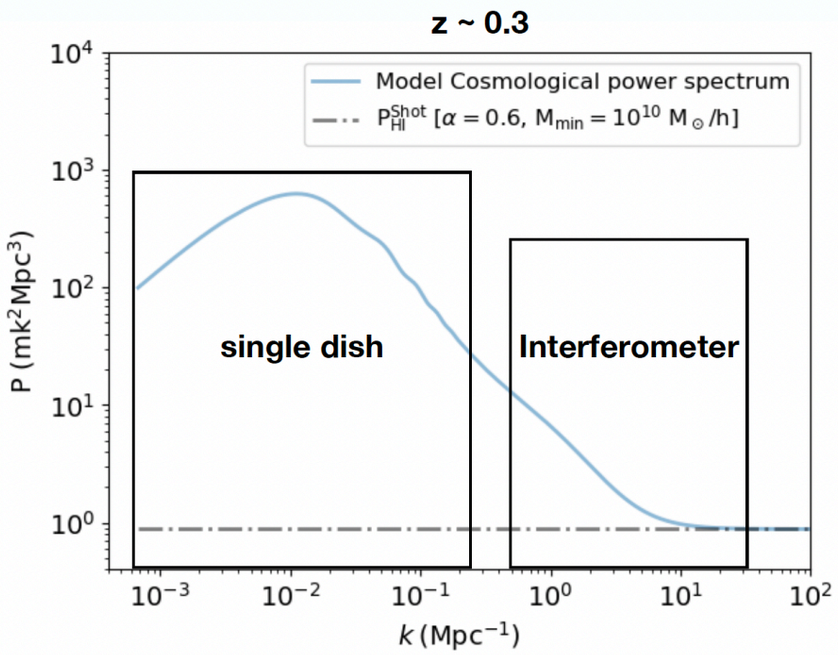

credit: Mario Santos

Ultimate aim MeerKLASS: MeerKAT Large Area Synoptic Survey, 4000 sq.deg

HI intensity mapping with MeerKAT

[Paul+ (2023)]

Power spectrum detected in cross-correlation with WiggleZ galaxies

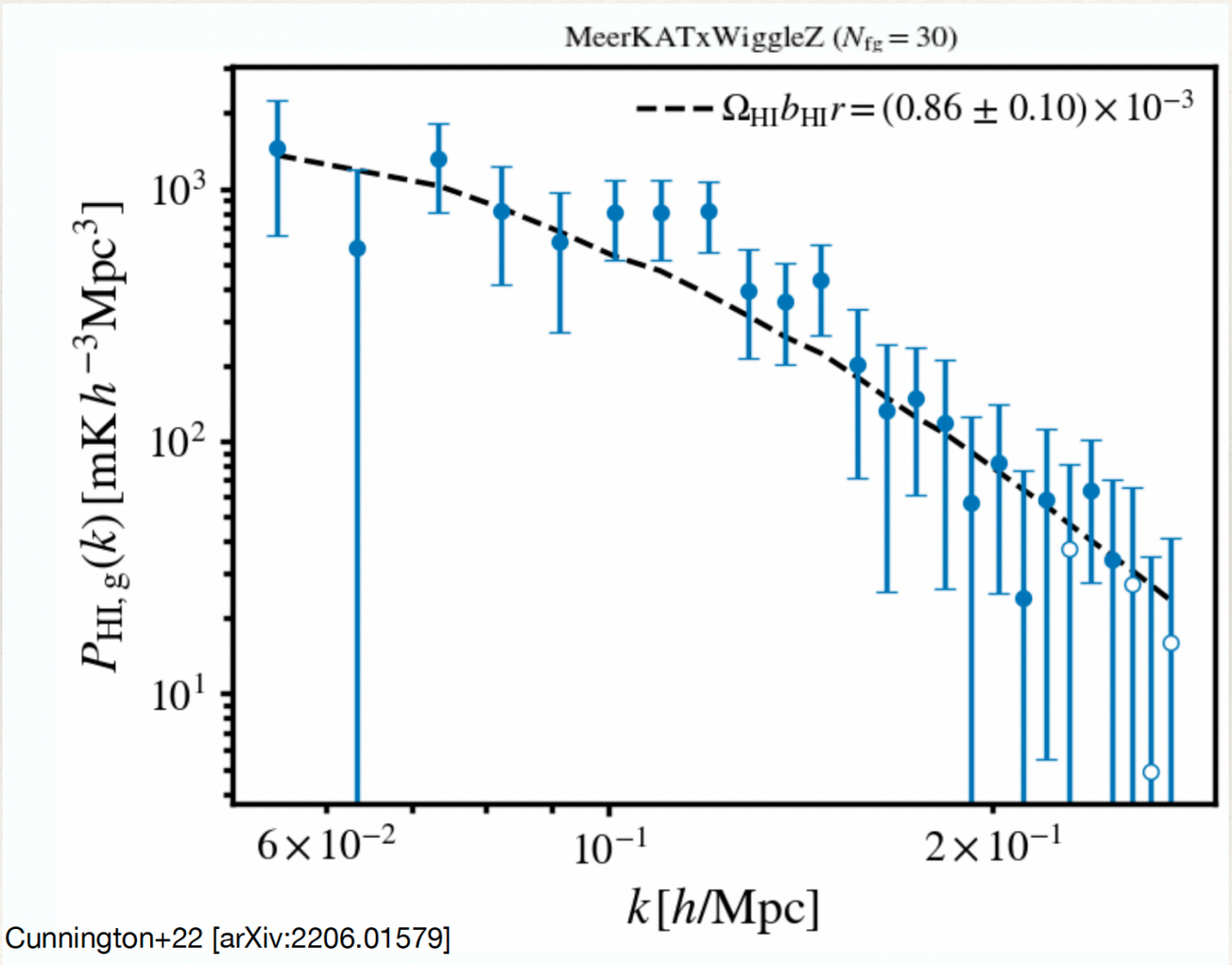

Cunnington+22 [arXiv:2206.01579]

credit: Steve Cunnington

Auto-correlation power detected for the first time to very small scales

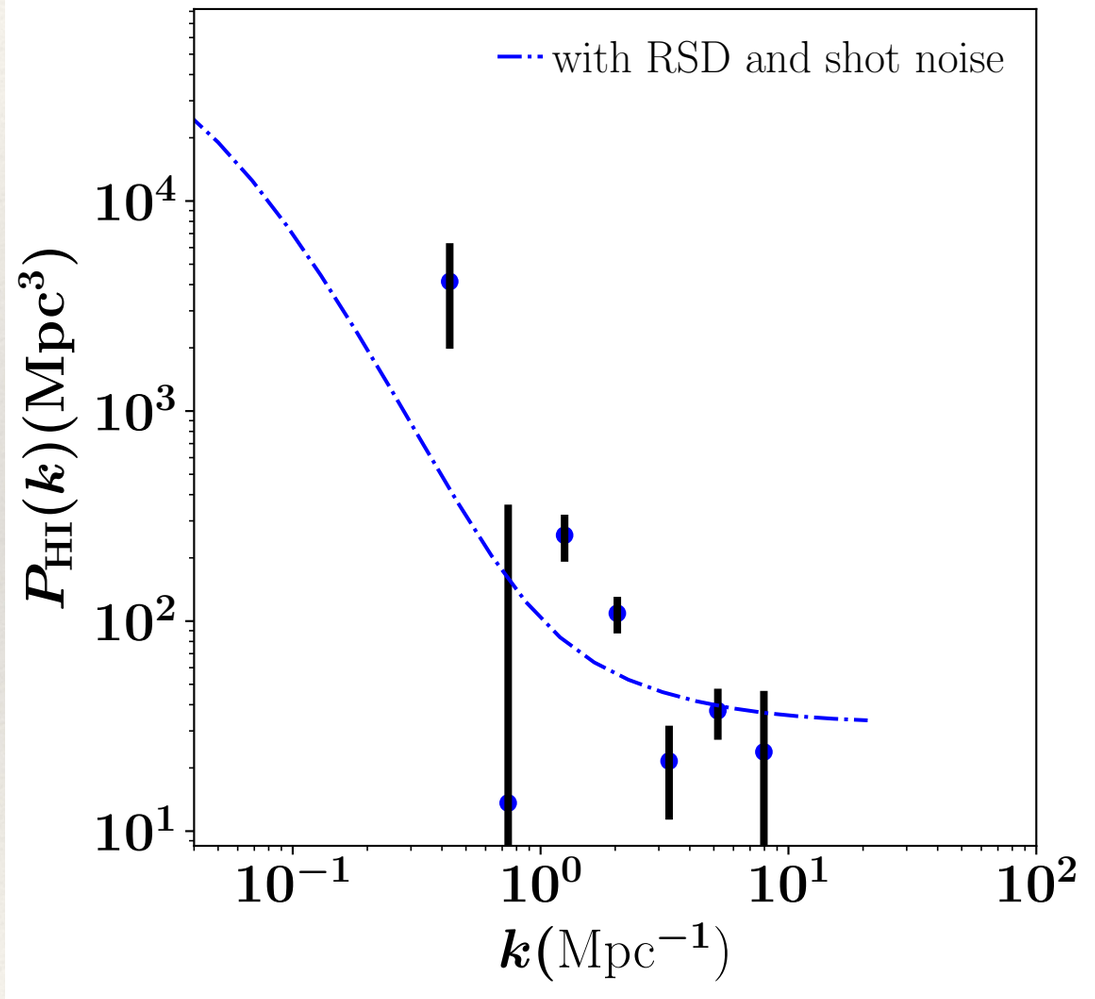

Requires modelling of small scale effects

Step 1: HI mass - halo mass relation

Matching data abundances to dark matter haloes

[Paul+ (2023), MeerKAT]

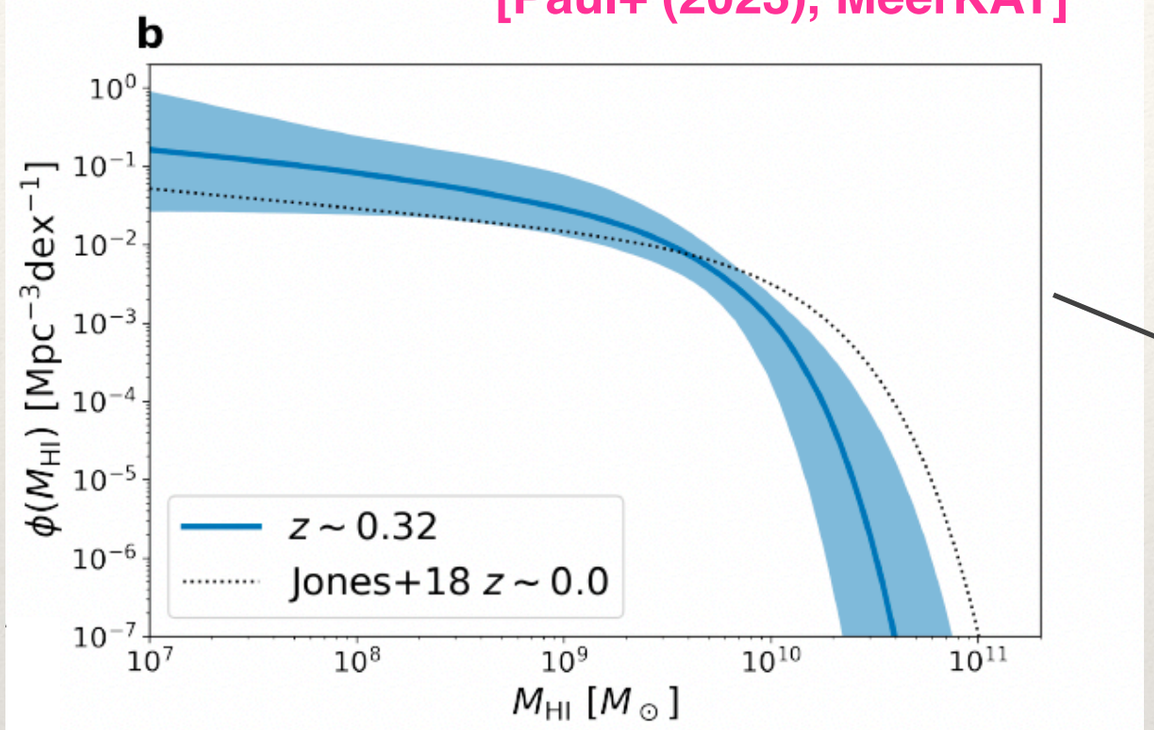

HI - halo mass already consistent with the halo model in present form

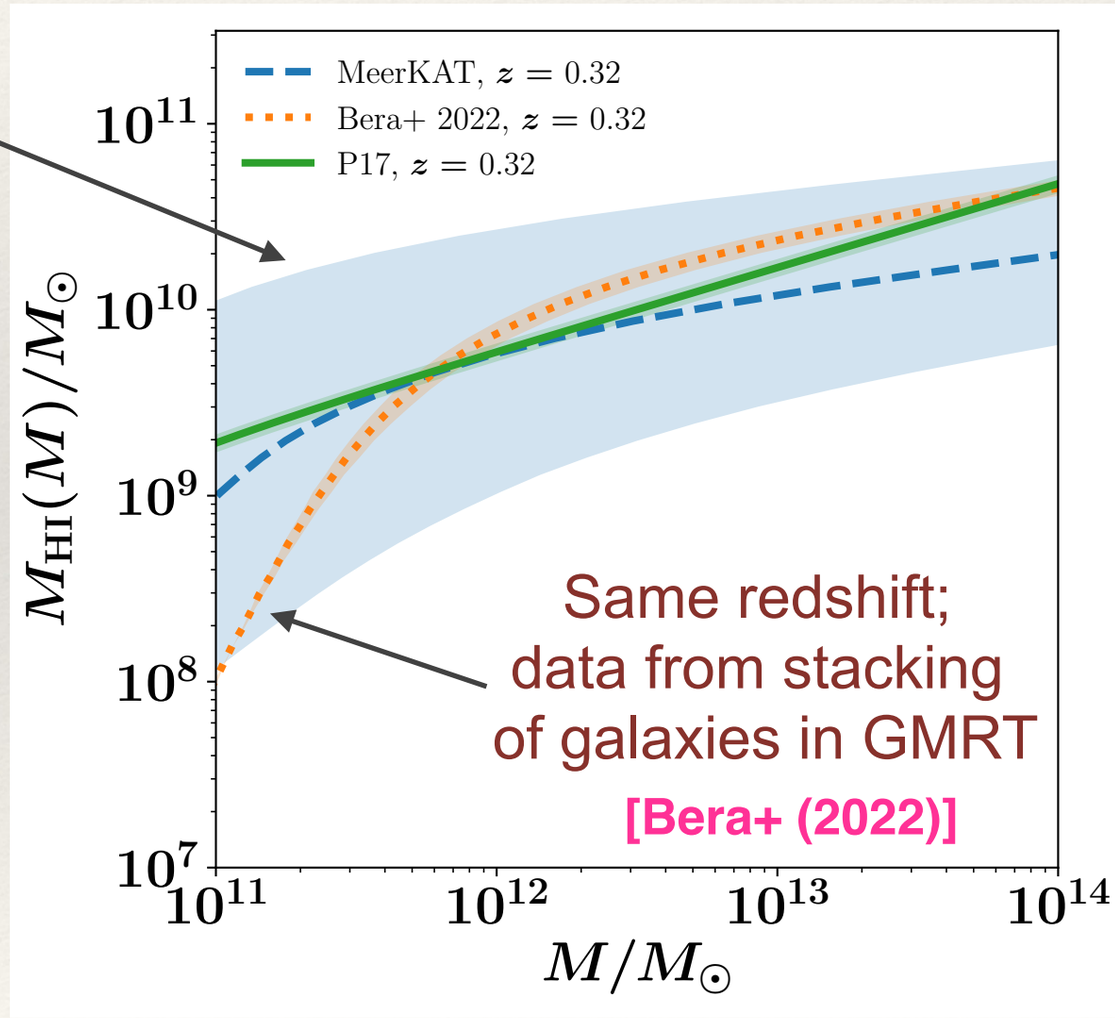

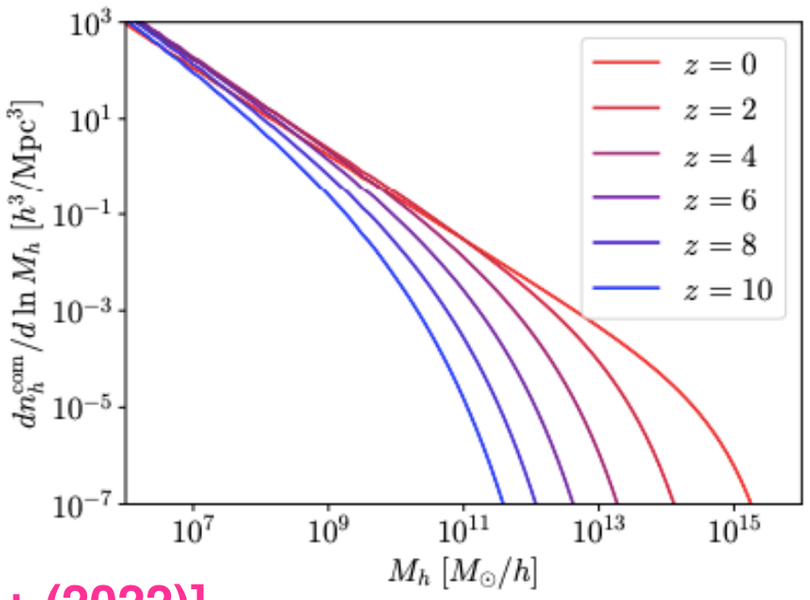

[Cui+ (2022)]

Dark matter halo abundance

Redshift space HI halo model

[HP (2021), HP+ (2023)]

$$P_{\rm 1h,HI}(k) = \frac{1}{\bar{\rho}_{\rm HI}^2}\int dM\, n(M) M_{\rm HI}^2 \left| u_{\rm HI}(k\,|\,M)\right|^2$$

$$P_{\rm 2h,HI}(k) = P_{\rm lin}(k)\left[\frac{1}{\bar{\rho}_{\rm HI}}\int dM\; n(M)\; M_{\rm HI}(M) b_{\rm h}(M) \left| u_{\rm HI}(k\,|\,M)\right|\right]^2,$$

Redshift space HI halo model

[HP (2021), HP+ (2023)]

$$P_{\rm 1h,HI}(k) = \frac{1}{\bar{\rho}_{\rm HI}^2}\int dM\, n(M) M_{\rm HI}^2 \left| u_{\rm HI}(k\,|\,M)\right|^2 \quad \text{+SN}$$

Shot Noise

$$P_{\rm 2h,HI}(k) = P_{\rm lin}(k)\left[\frac{1}{\bar{\rho}_{\rm HI}}\int dM\; n(M)\; M_{\rm HI}(M) b_{\rm h}(M)\left| u_{\rm HI}(k\,|\,M)\right|\right]^2,$$

$$\delta^{\rm s}_{\rm HI}(\mathbf{k}) = \delta_{\rm HI} + f\mu^2\delta_{\rm h}\;;\; \delta^{\rm s}_{\rm HI} \to \delta^{\rm s}_{\rm HI}\exp\left(-\frac{1}{2}k^2\mu^2\sigma^2\right)$$

Kaiser effect

Finger-of-God effect

$$\bar{P}^{\rm s}_{\rm HI}(k) = \left(F_{\rm HI}^2 + \frac{2}{3}F_{\rm m}F_{\rm HI} + \frac{1}{5}F_{\rm m}^2\right)P_{\rm lin}(k) + \frac{1}{\bar{\rho}_{\rm HI}^2}\int dM\, n(M) M_{\rm HI}^2\, \mathscr{R}_2(k\sigma)\left| u_{\rm HI}(k,M)\right|^2,$$

Kaiser effect

$$F_{\rm m} = \frac{f}{\bar{\rho}_m}\int dM\, M\; n(M) b_{\rm h}(M)\, \mathscr{R}_1(k\sigma) u_{\rm h}(k,M),$$

Finger-of-God effect

$$F_{\rm HI} = \frac{1}{\bar{\rho}_{\rm HI}}\int dM\, n(M) M_{\rm HI}(M) b_{\rm h}(M)\, \mathscr{R}_1(k\sigma) u_{\rm HI}(k,M)\;.$$

Consistent with the Parkes data

[HP (2021) IJMPD, arXiv:2109.00003]

$$\bar{P}^{\rm s}_{\rm HI}(k) = \left(F^2_{\rm HI} + \frac{2}{3}F_{\rm m}F_{\rm HI} + \frac{1}{5}F^2_{\rm m}\right) P_{\rm lin}(k) + \frac{1}{\bar{\rho}^2_{\rm HI}} \int dM\, n(M) M^2_{\rm HI}\, \mathscr{R}_2(k\sigma) \left| u_{\rm HI}(k, M) \right|^2 ,$$

Galaxy bias ~ 0.85; cross-correlation spectrum

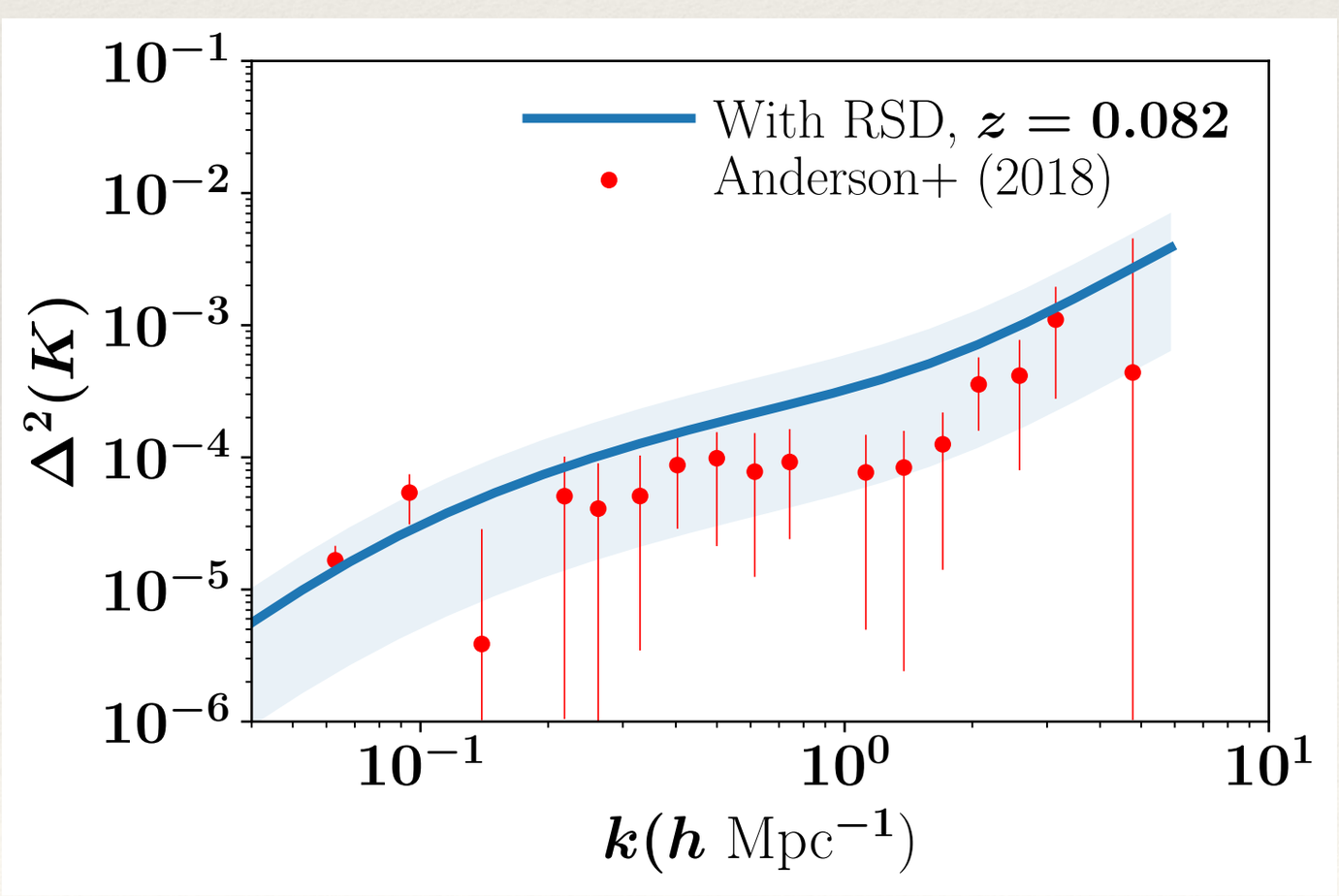

Step 2: Fitting to MeerKAT data

- Data goes to small scales, for the first time ~ 0.1 Mpc
- Halo model framework extended to include *Redshift Space Distortions, Kaiser and Finger-of-God* effects at small scales
- Predictions consistent at $z \sim 0.32$. At $z \sim 0.44$, evidence for greater amplitude of the power than predicted, different possible causes

$z \sim 0.32$

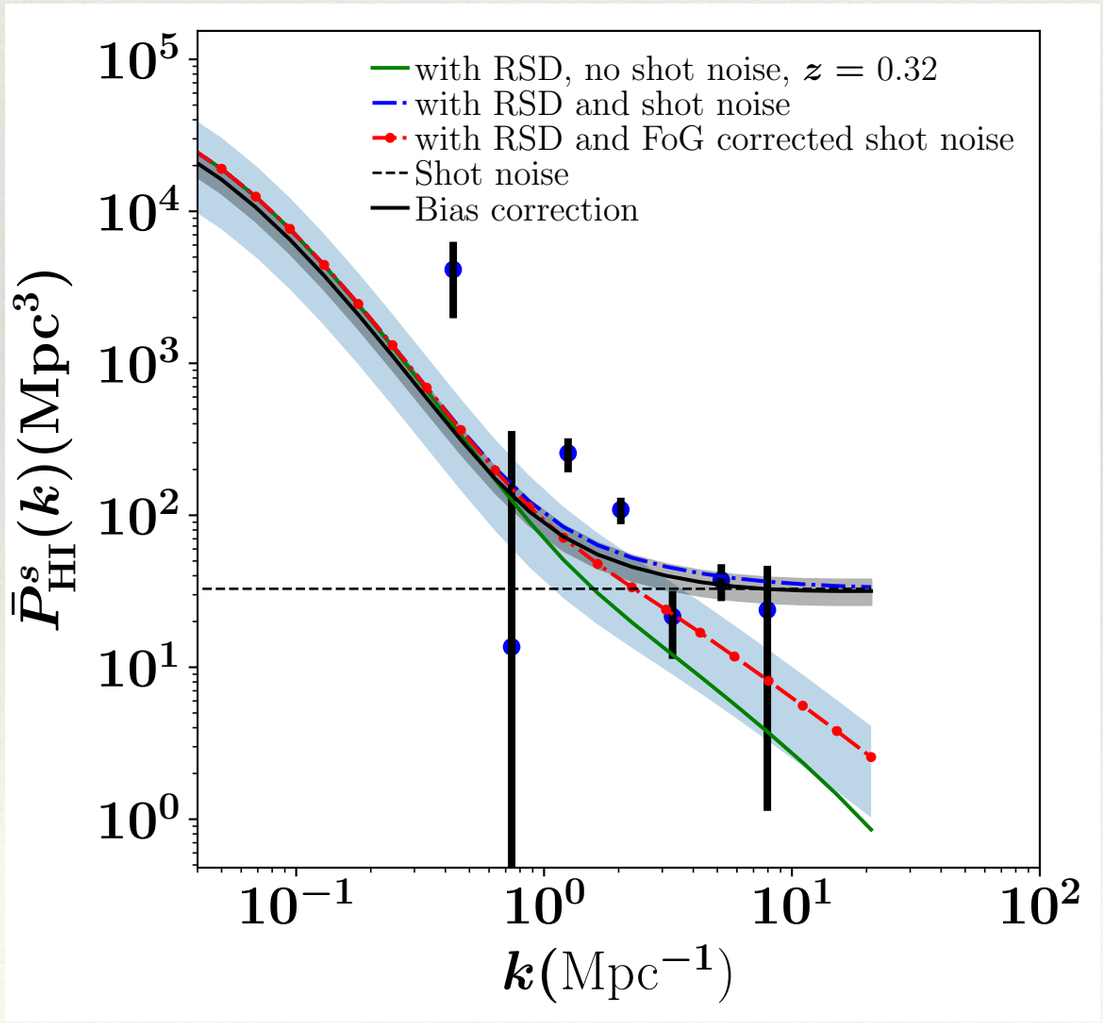

$z \sim 0.44$

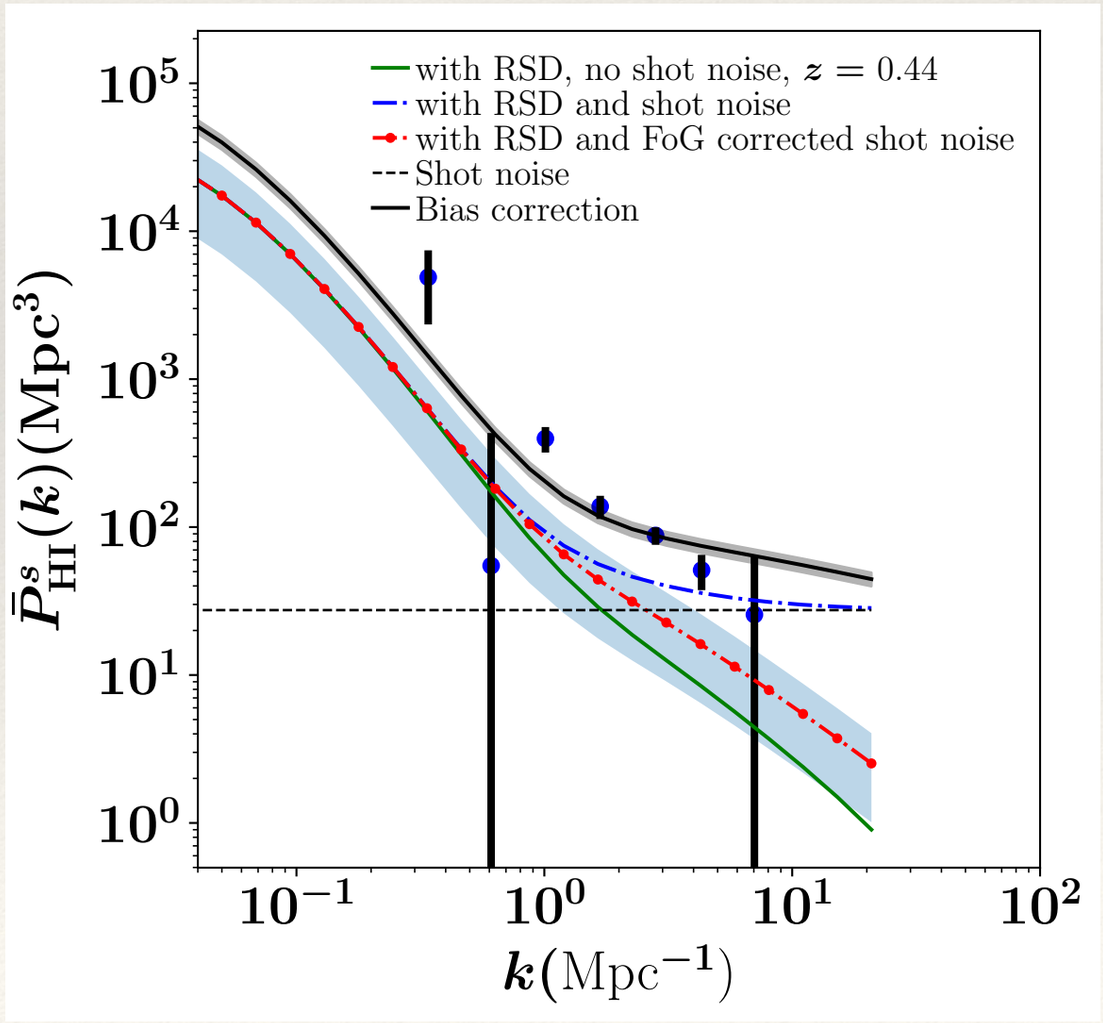

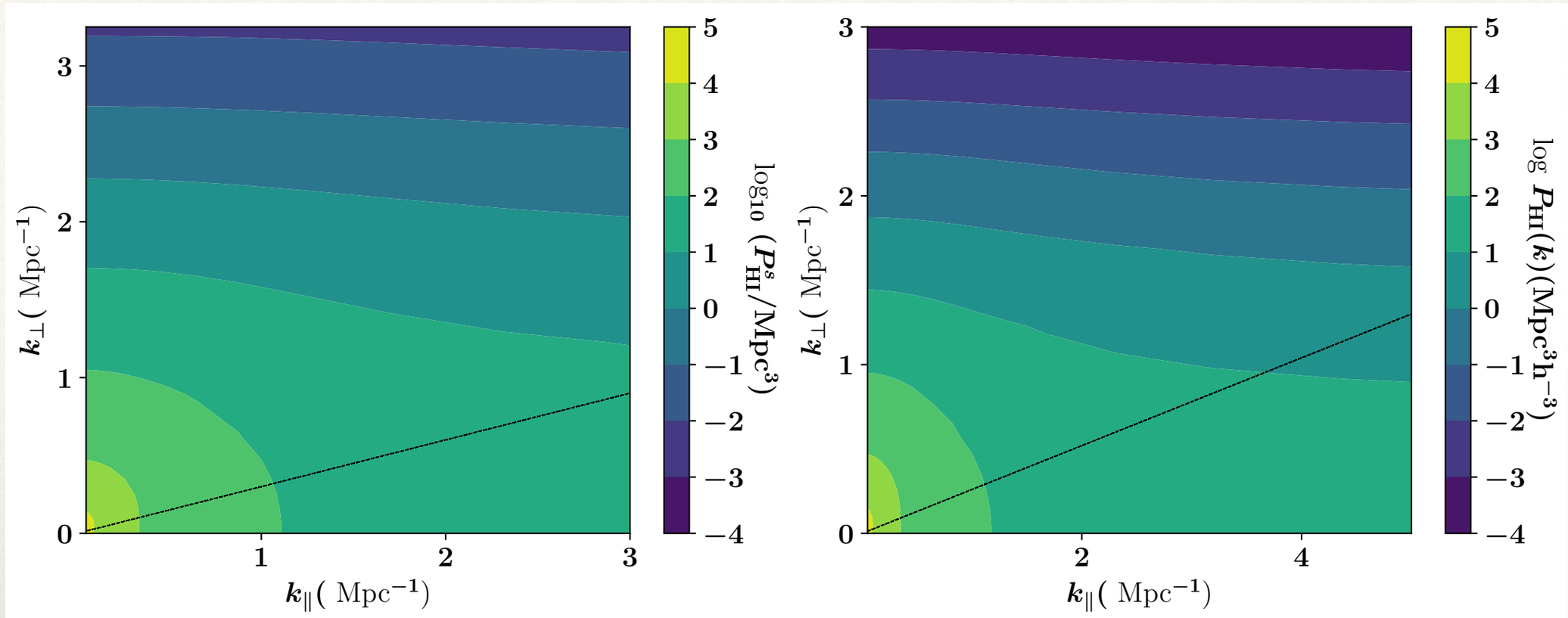
$k_\perp$ (Mpc^{-1})
$k_\parallel$ (Mpc^{-1})
$\log_{10}(P^s_{\rm HI}/{\rm Mpc}^3)$
$\log P_{\rm HI}(k)({\rm Mpc}^3{\rm h}^{-3})$

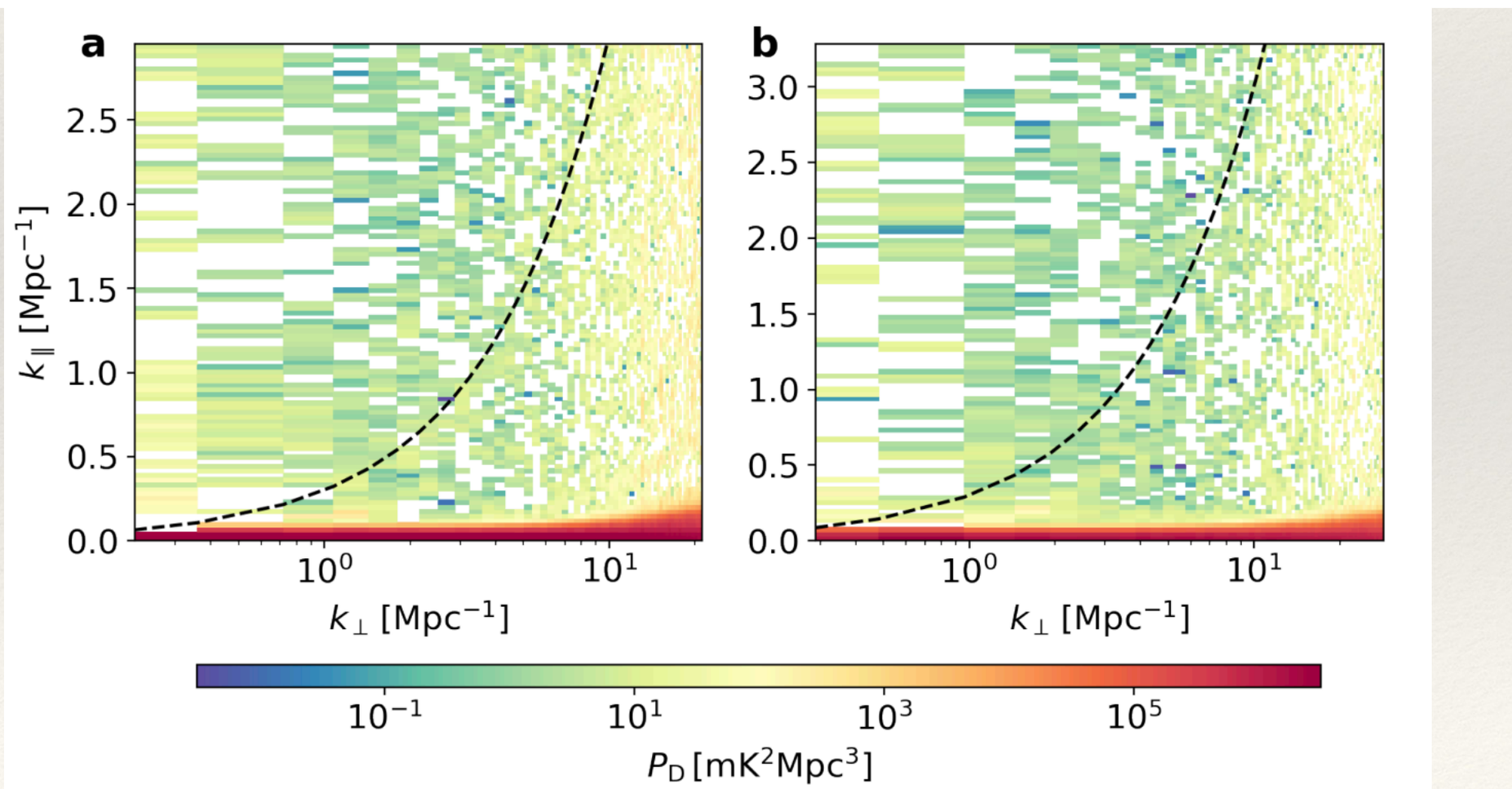
a
b
$k_\parallel$ [Mpc^{-1}]
$k_\perp$ [Mpc^{-1}]
$P_{\rm D}$ [mK^{2}Mpc^3]

21 cm IM is not easy …

Challenges to overcome with intensity mapping

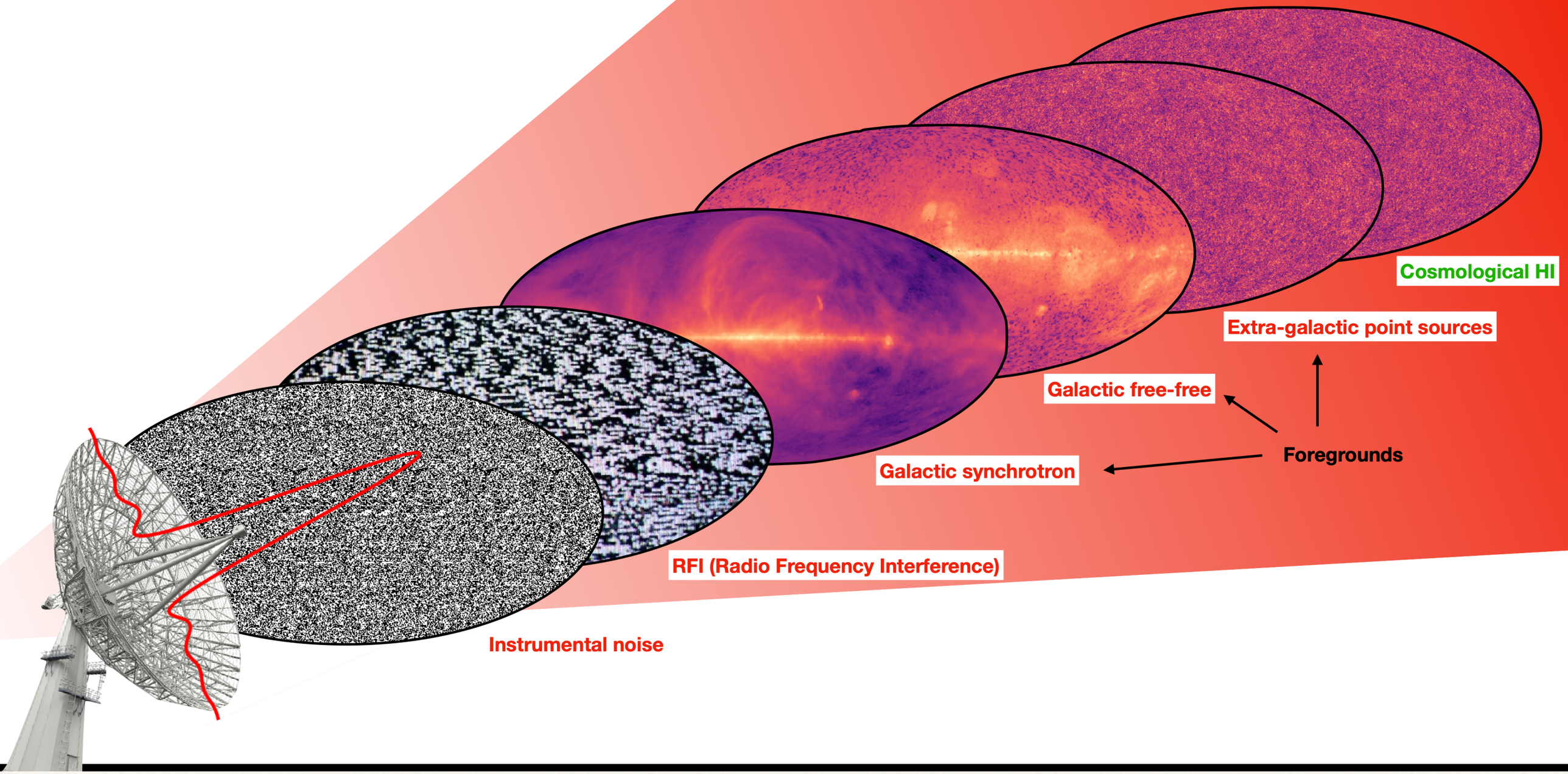

Slide credit: Steve Cunnington

Some first claimed detections …

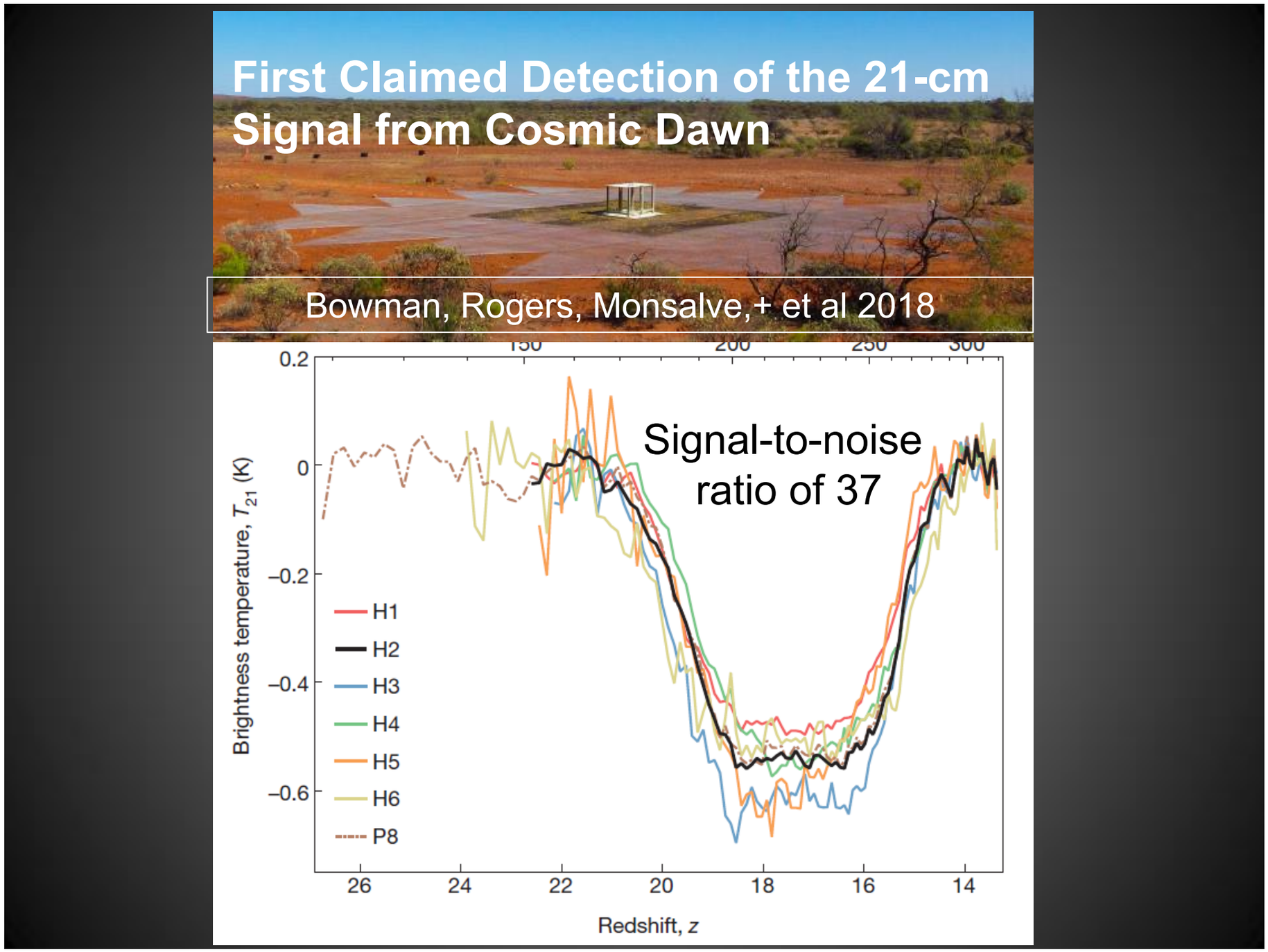

Slide credit: Anastasia Fialkov

… which, however, need to be confirmed …

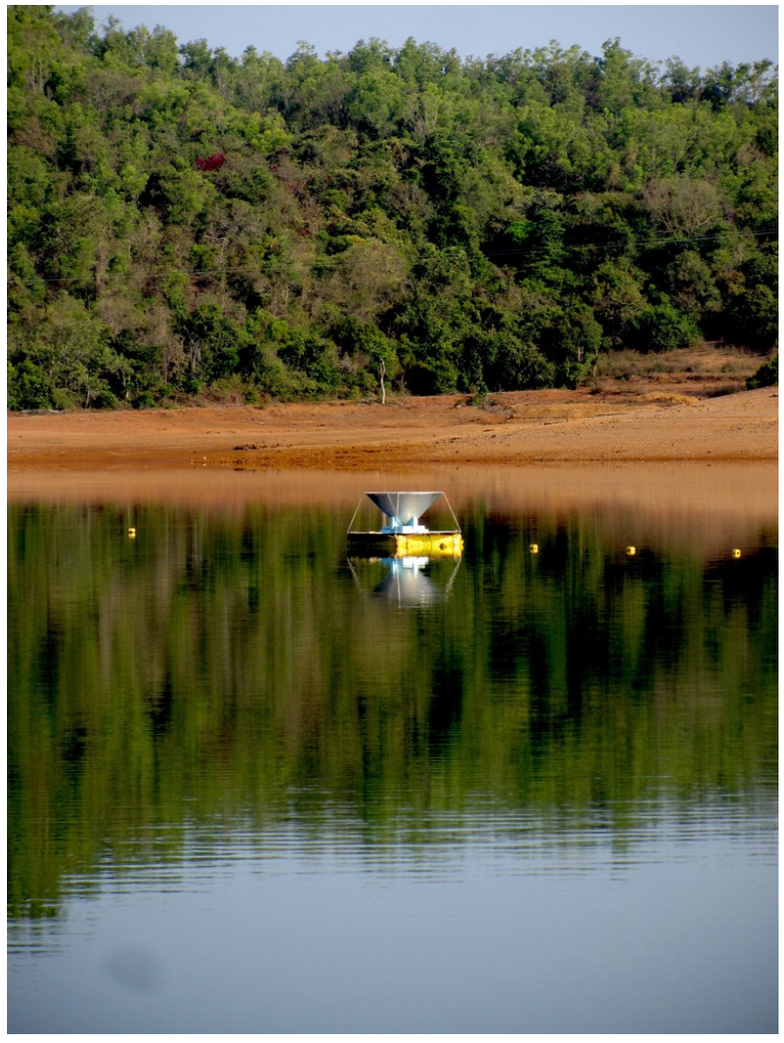

nature

Explore content | About the journal | Publish with us | Subscribe

nature > news > article

NEWS | 28 February 2022

Did astronomers see hints of first stars? Experiment casts doubt on bold claim

Radioastronomers suggest that a signal reported to be from the cosmic dawn could have been caused by instrument error.

nature astronomy

ARTICLES

https://doi.org/10.1038/s41550-022-01610-5

Check for updates

On the detection of a cosmic dawn signal in the radio background

Saurabh Singh[1,2,3] ✉, Jishnu Nambissan T.[1,4], Ravi Subrahmanyan[1,5], N. Udaya Shankar[1], B. S. Girish[1], A. Raghunathan[1], R. Somashekar[1], K. S. Srivani[1] and Mayuri Sathyanarayana Rao[1]

The astrophysics of the cosmic dawn, when star formation commenced in the first collapsed objects, is predicted to be revealed by spectral and spatial signatures in the cosmic radio background at long wavelengths. The sky-averaged redshifted 21 cm absorption line of neutral hydrogen is a probe of the cosmic dawn. The line profile is determined by the evolving thermal state of the gas, radiation background, Lyman α radiation from stars scattering off cold primordial gas, and relative populations of the hyperfine spin levels in neutral hydrogen atoms. We report a radiometer measurement of the spectrum of the radio sky in the 55–85 MHz band, which shows that the profile found by Bowman et al. in data taken with the Experiment to Detect the Global Epoch of Reionization Signature (EDGES) low-band instrument is not of astrophysical origin; their best-fitting profile is rejected with 95.3% confidence. The profile was interpreted to be a signature of the cosmic dawn; however, its amplitude was substantially higher than that predicted by standard cosmological models. Our non-detection bears out earlier concerns and suggests that the profile found by Bowman et al. is not evidence for new astrophysics or non-standard cosmology.

Cross-correlations with 21 cm

Cross-correlations mitigate systematics

Radio

MeerKAT radio telescope

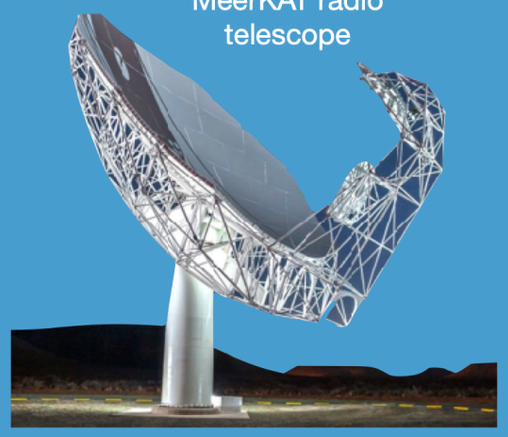

$$\mathbf{X}_{\rm rad} = \mathbf{S}_{\rm rad} + \mathbf{N}_{\rm rad}$$

Optical

Anglo-Austrailian Observatory

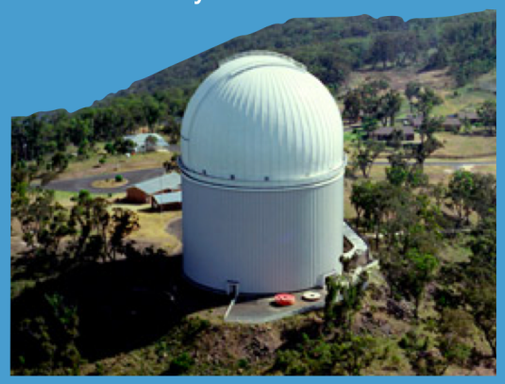

$$\mathbf{X}_{\rm opt} = \mathbf{S}_{\rm opt} + \mathbf{N}_{\rm opt}$$

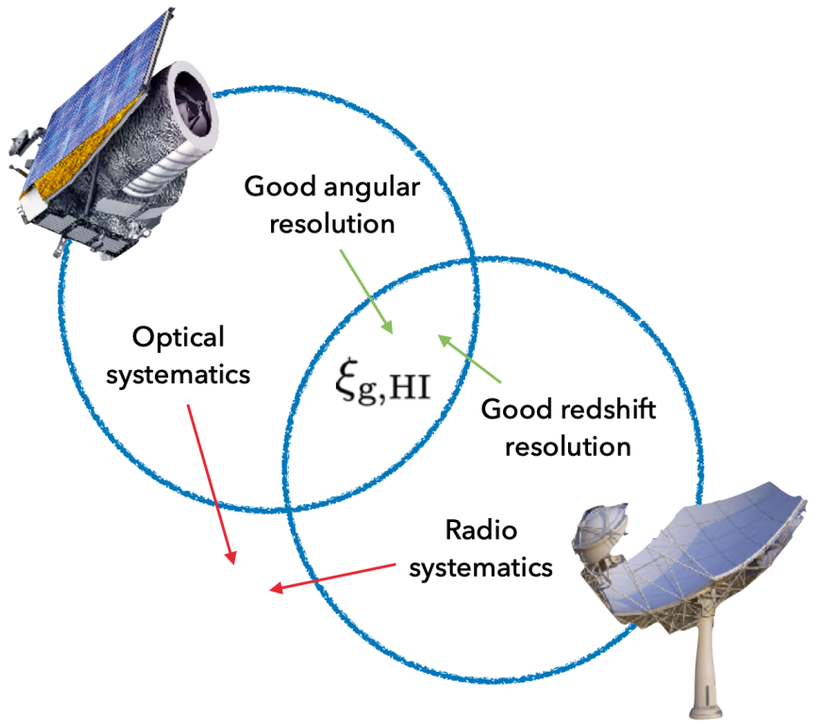

Auto Correlation:

$$\langle \mathbf{X}_{\rm rad}\mathbf{X}_{\rm rad}\rangle = \langle \mathbf{S}_{\rm rad}\mathbf{S}_{\rm rad}\rangle + 2\langle \mathbf{S}_{\rm rad}\mathbf{N}_{\rm rad}\rangle + \langle \mathbf{N}_{\rm rad}\mathbf{N}_{\rm rad}\rangle$$

uncorrelated

$$\langle \mathbf{X}_{\rm rad}\mathbf{X}_{\rm rad}\rangle = \langle \mathbf{S}_{\rm rad}\mathbf{S}_{\rm rad}\rangle + \langle \mathbf{N}_{\rm rad}\mathbf{N}_{\rm rad}\rangle$$

signal you want — *noise/residuals/systematics you don't want*

Cross Correlation:

$$\langle \mathbf{X}_{\rm opt}\mathbf{X}_{\rm rad}\rangle = \langle \mathbf{S}_{\rm opt}\mathbf{S}_{\rm rad}\rangle + \langle \mathbf{S}_{\rm opt}\mathbf{N}_{\rm rad}\rangle + \langle \mathbf{S}_{\rm rad}\mathbf{N}_{\rm opt}\rangle + \langle \mathbf{N}_{\rm opt}\mathbf{N}_{\rm rad}\rangle$$

21cm intensity mapping will provide benefits in future cross-correlations

Slide credit: Steve Cunnington

Cross-correlation with galaxy survey < few sq. deg.: information loss in areas most affected by foregrounds
Mitigated by using IM with e.g. [CII], covering ~ few ten square degrees or more

[Lidz+ (2009), Beane & Lidz (2018), Beane et al. (2019)]

Intensity mapping in the sub-mm

[reviews: Kovetz+ (2019), Karkare+ (2022), Bernal & Kovetz (2022)]

- Novel window into reionization, sensitive to evolution of star-formation rate and molecular gas density
- [CII] brightest line, ~ 1% of total IR luminosity, non-affected by dust and photodissociation (caveat: CO transitions at lower redshift a possible contaminant, but can be mitigated, especially by cross-correlation)
- [OIII]: hard radiation > 35 eV; HII regions
- ALMA observations: [CII] ‘deficit’ at high-z; if confirmed by IM, indicates hard ISM field and/or larger HII regions
- Sky noise much smaller at 10-100 GHz
- Point source foregrounds at ~ 30 GHz effectively removed

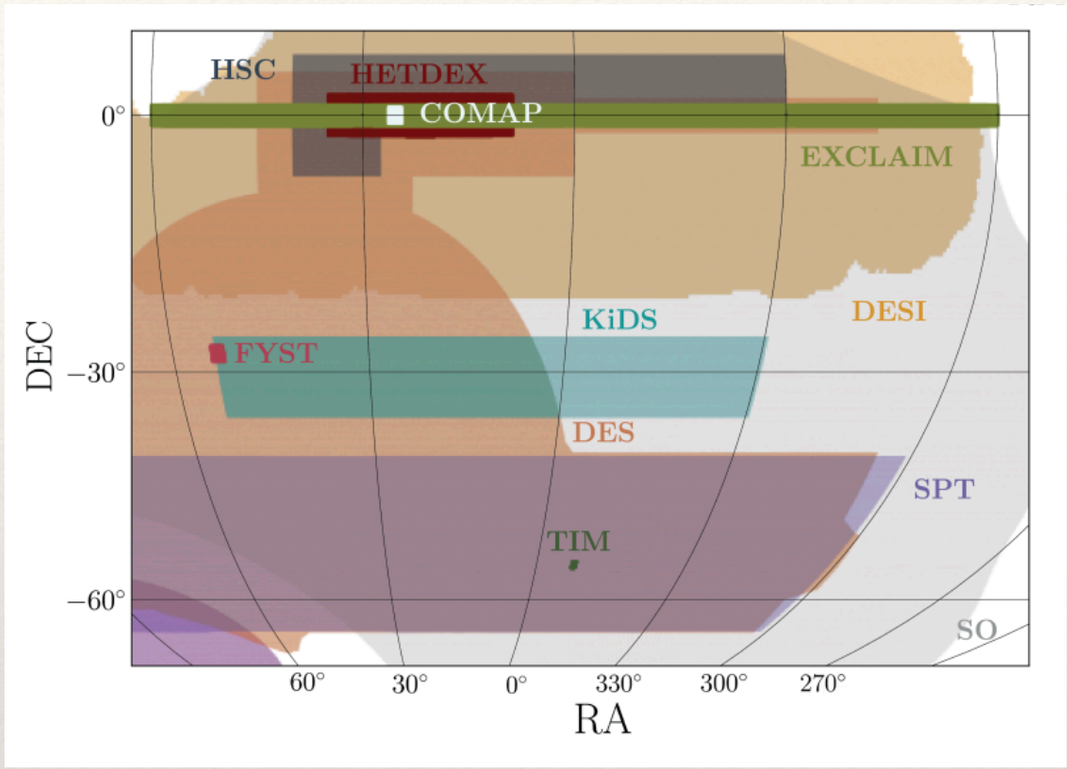

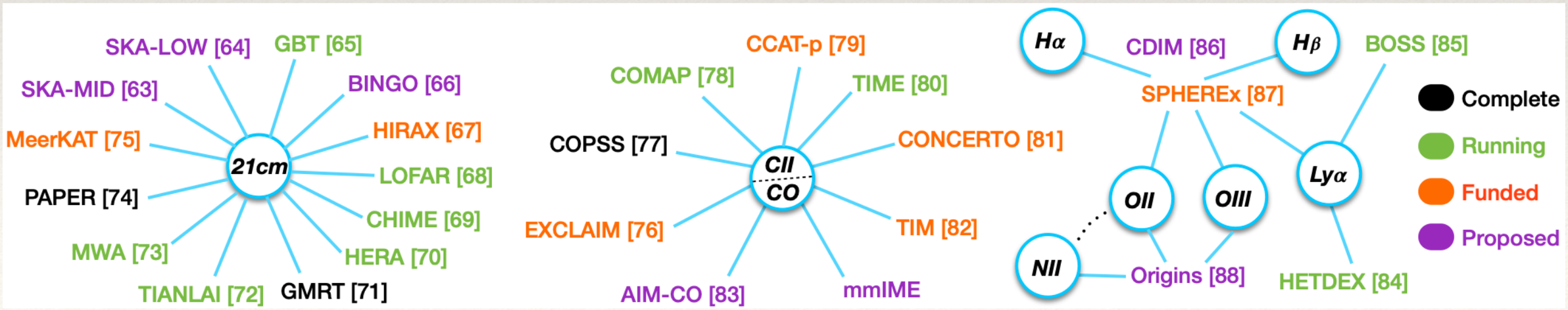

Intensity mapping in the sub-mm

Experiment for Cryogenic Large Aperture Intensity Mapping (EXCLAIM)

(2024 -)

[Cataldo+ (2020), SPIE, arXiv:2101.11734; Ade+ (2020), JLTP, arXiv:1912.07118]

EoR-Spec on Fred Young Submillimetre Telescope (FYST)

(2025 -)

[Aravena+ (2021), arXiv:2107.10364; Duell+ (2020), SPIE, arXiv: 2012.10411]

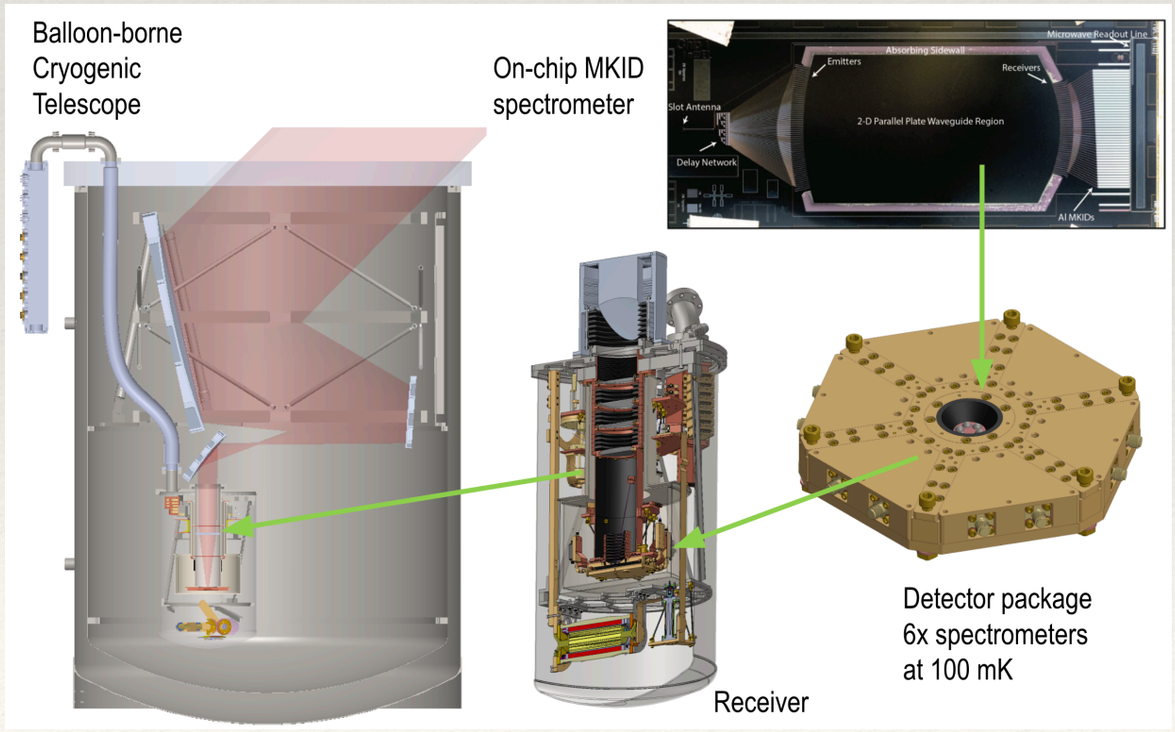

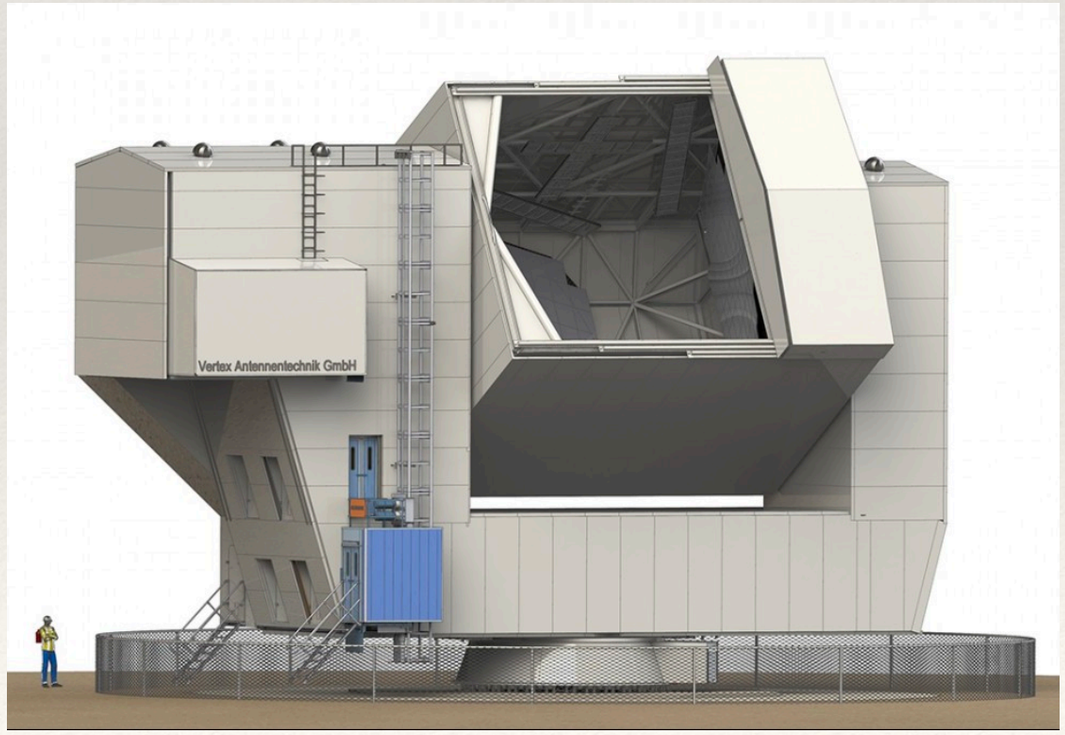

The ALPINE and REBELS surveys: constraints on high-z [CII] LF

- ALPINE: [CII] emission in galaxies at z ~ 4.5 - 6 in Chandra Deep Field South and COSMOS fields
  [Le Fèvre et al. (2020), Faisst et al. (2020), Bethermin et al. (2020)]
- Targeted and serendipitous sources, ‘clustered’ subsample connected to known overdensities in the COSMOS field
  [Loiacono+ (2021), Oesch+ (2022)]
- REBELS: 42 sources, spectroscopic redshifts z ~ 6.4 - 7.7 **[Oesch+ (2022)]**
- [CII] luminosity to host halo mass found by abundance matching to dark matter mass function
  [HP (MNRAS, 2023), arXiv:2212.08077, HP (MNRAS 2019)]

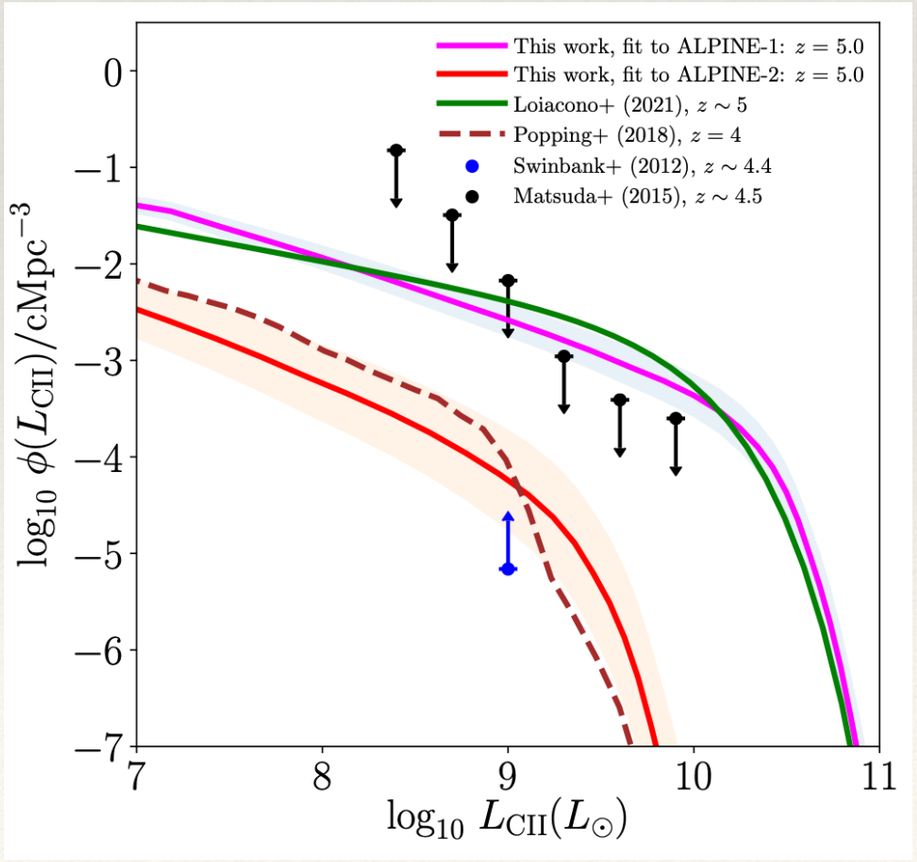

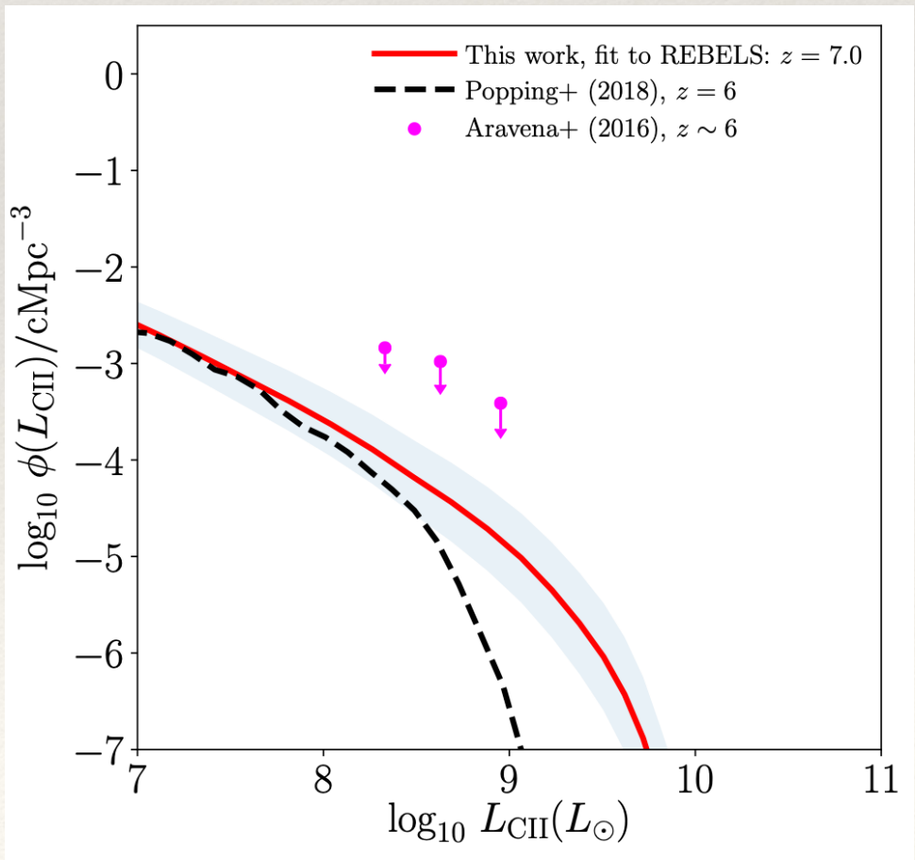

New empirical insights on HI at z ~ 5-7

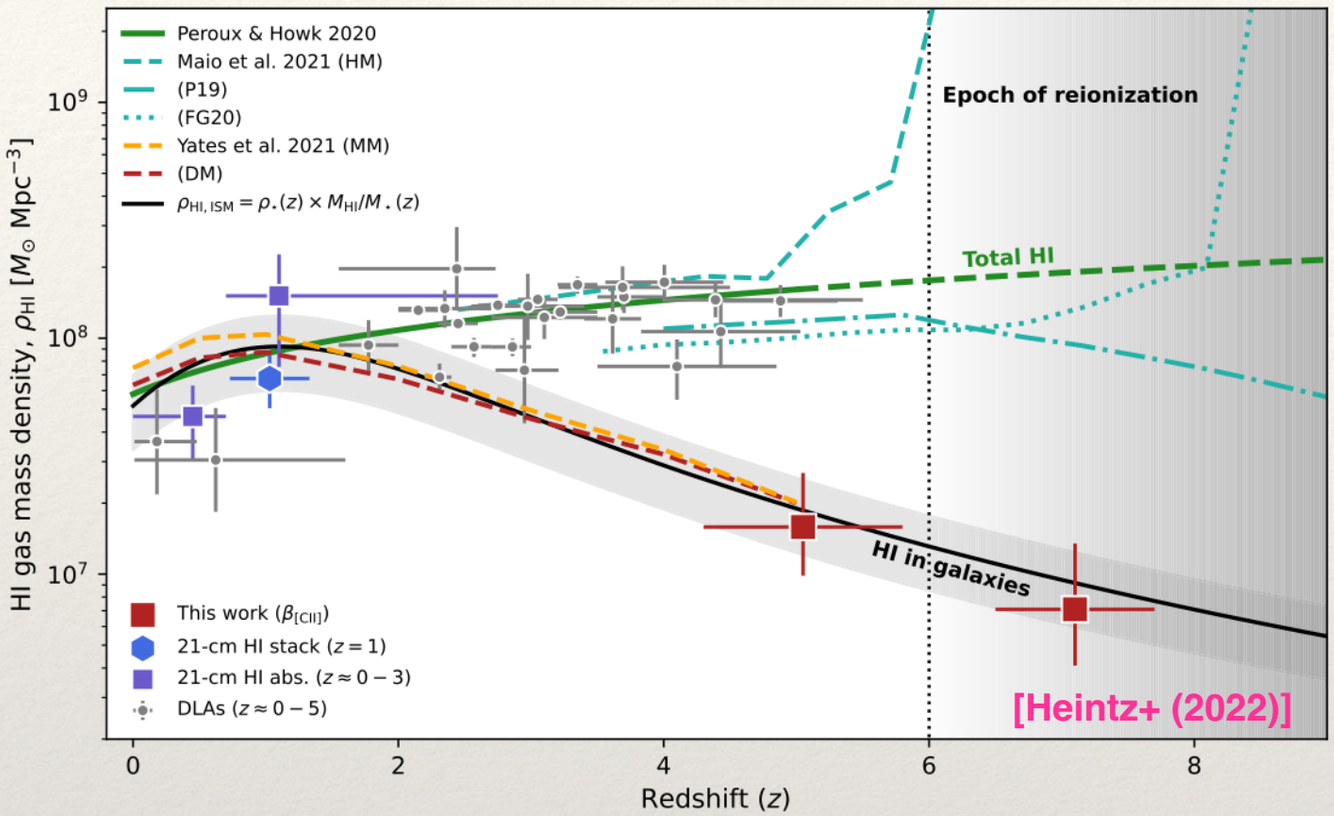

[Heintz+ (2022)]

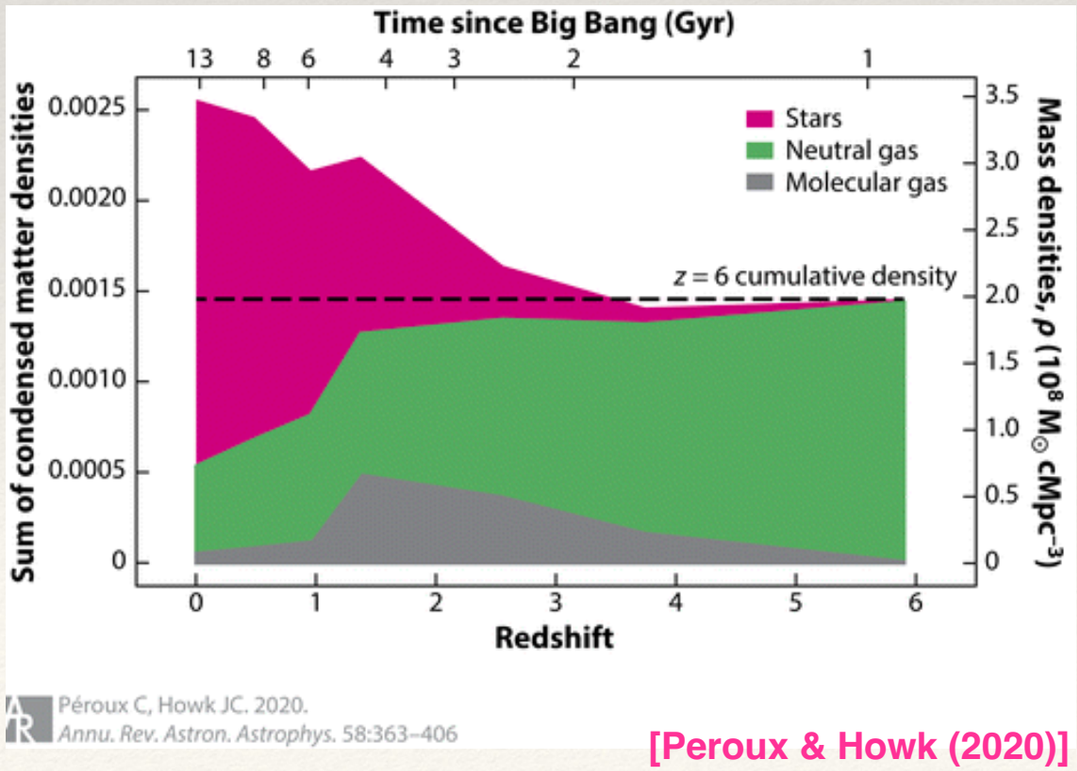

[Peroux & Howk (2020)]

Consistent with the HI halo model in its present form!*

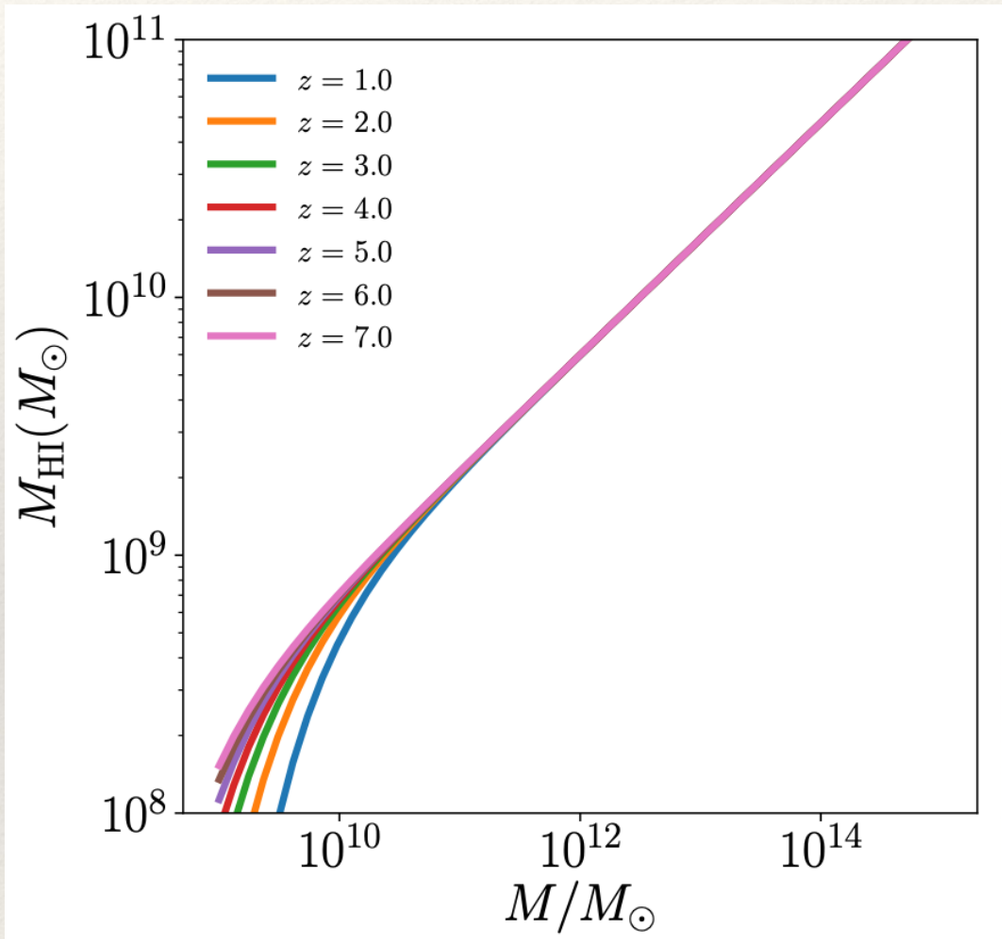

[HP, Refregier, Amara, MNRAS (2017)]

**Note: total power only, scale dependence unconstrained*

Auto-correlation forecasts

MWA/SKA, z ~ 6-7

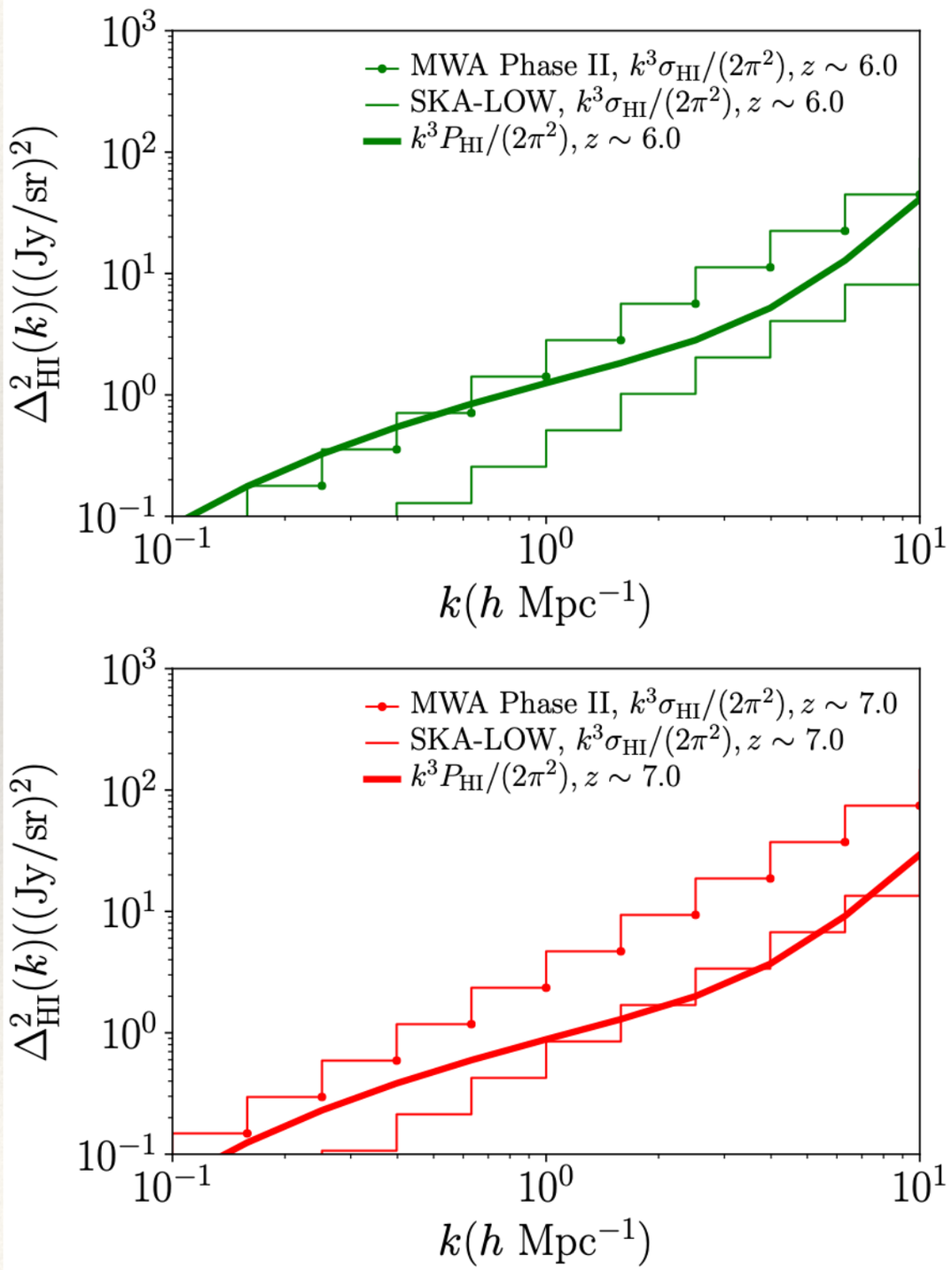

Configuration	$d_{\rm max}$	$N_{\rm a}$	$n_{\rm pol}$	$T_{\rm inst}$[K]	$A_{\rm eff}$ (m^2)	$t_{\rm obs}$[h]	$S_{\rm A}$[deg.sq]
MWA	1000 m	256	2	28	14.5	2000	1000
SKA-LOW	40000 m	512	2	28	964	2000	1000

FYST++, z ~ 6

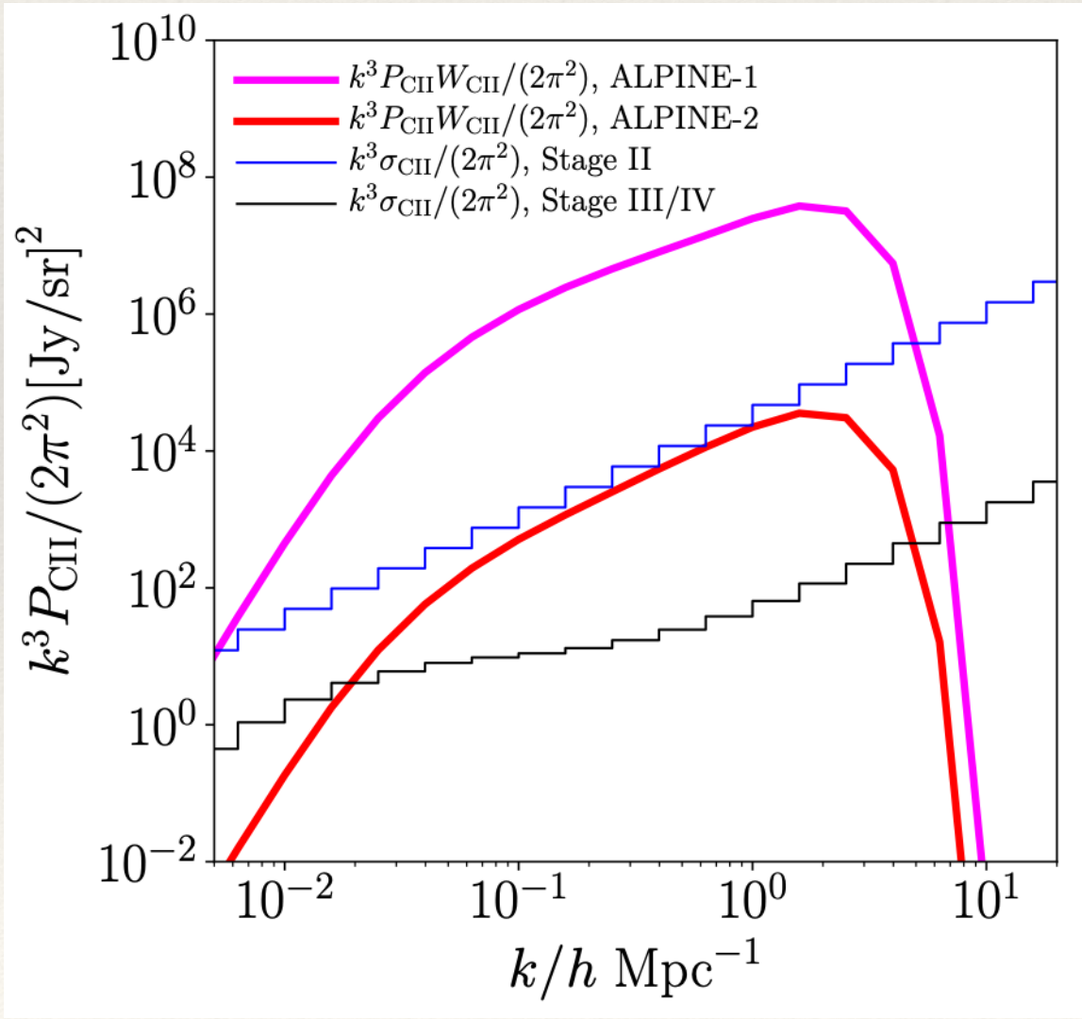

Cross-correlations of sub-mm & 21 cm

- high redshifts -

**Assumes complete overlap*

(FYST++) x MWA/SKA

z ~ 5.5-6.5, [CII] 158 x HI (MWA)

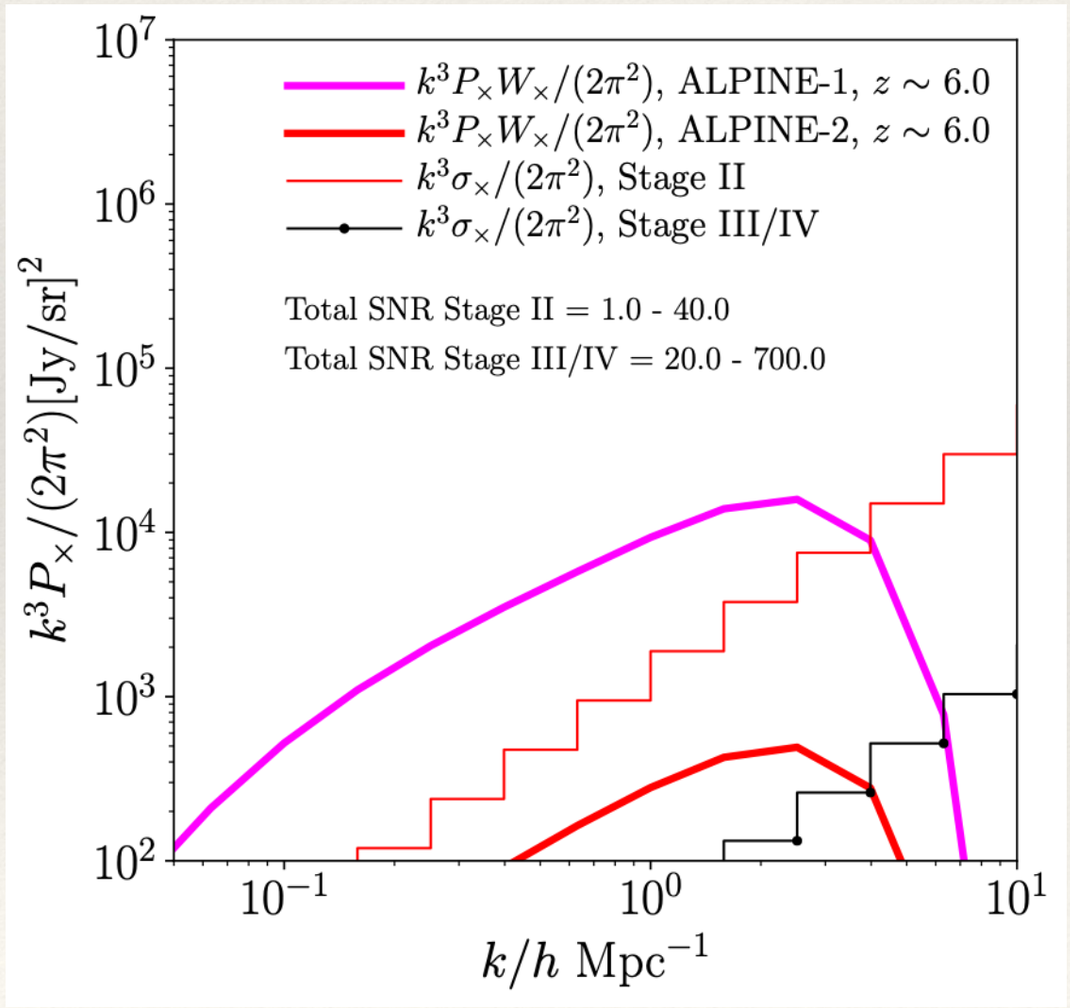

z ~ 7, [CII] 158 x HI (MWA)

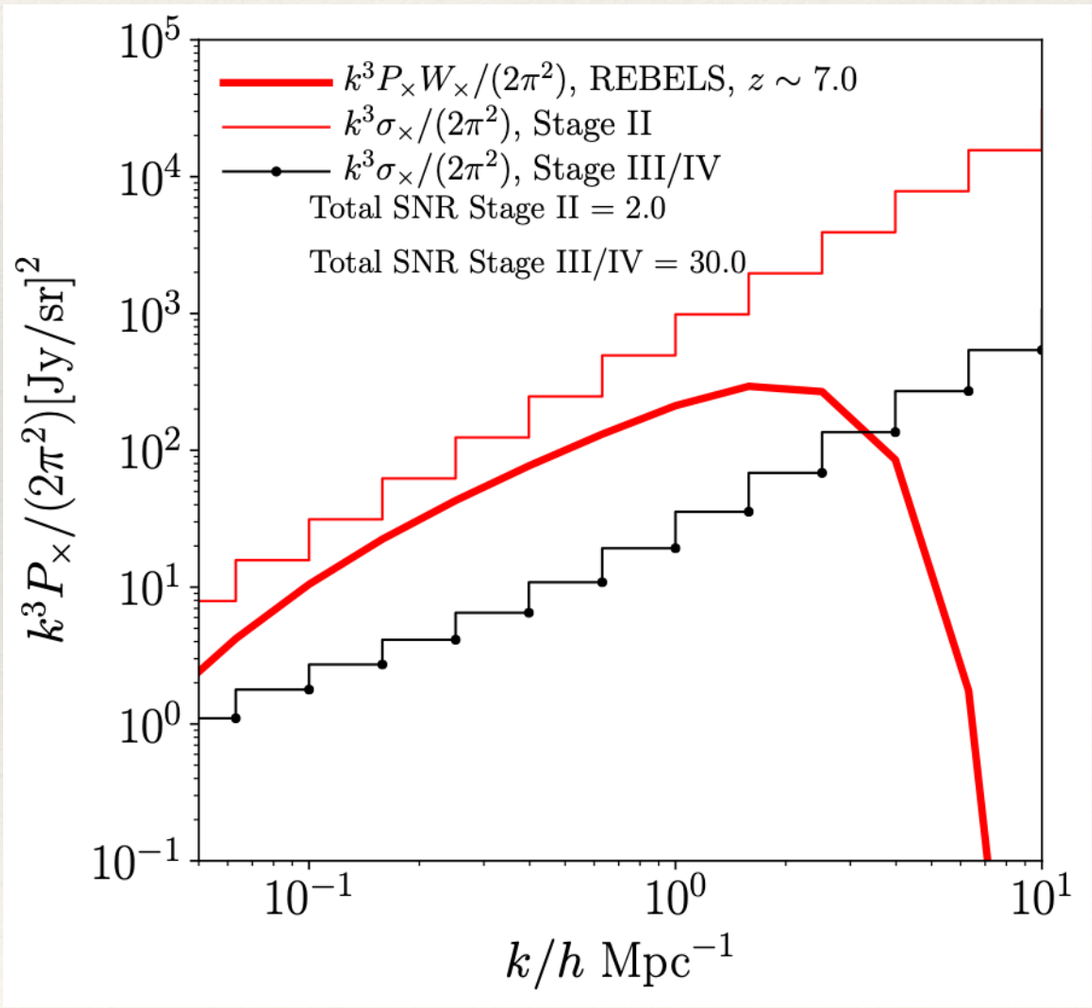

[HP (MNRAS, 2018), HP (MNRAS 2019), HP+ (MNRAS 2022), HP (MNRAS 2023, arXiv:2212.08077)]

Cross-correlations of sub-mm & 21 cm

- high redshifts -

**Assumes complete overlap*

(EXCLAIM++) x MWA/SKA

z ~ 5.5-6.5, [OIII] 88 x HI (MWA)

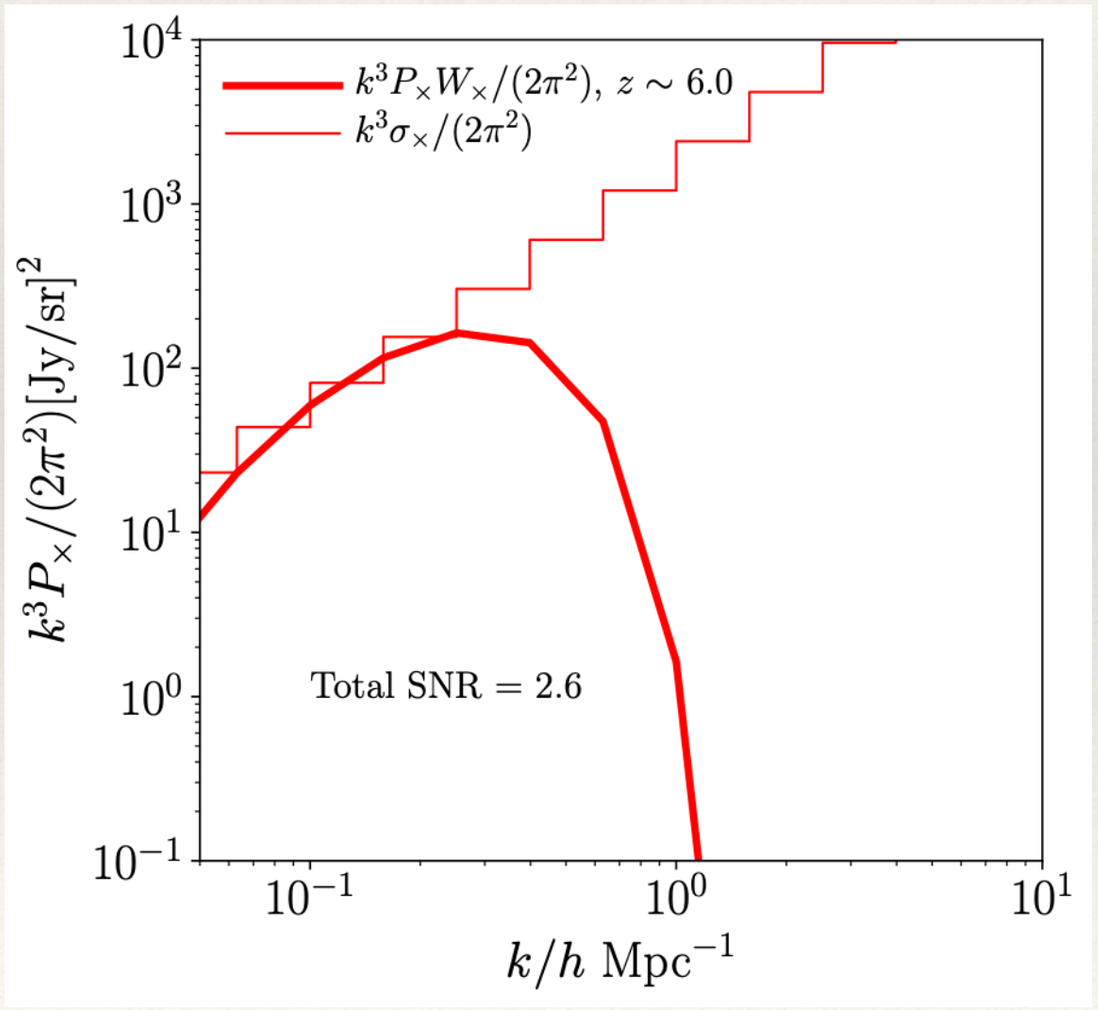

z ~ 7, [OIII] 88 x HI (MWA)

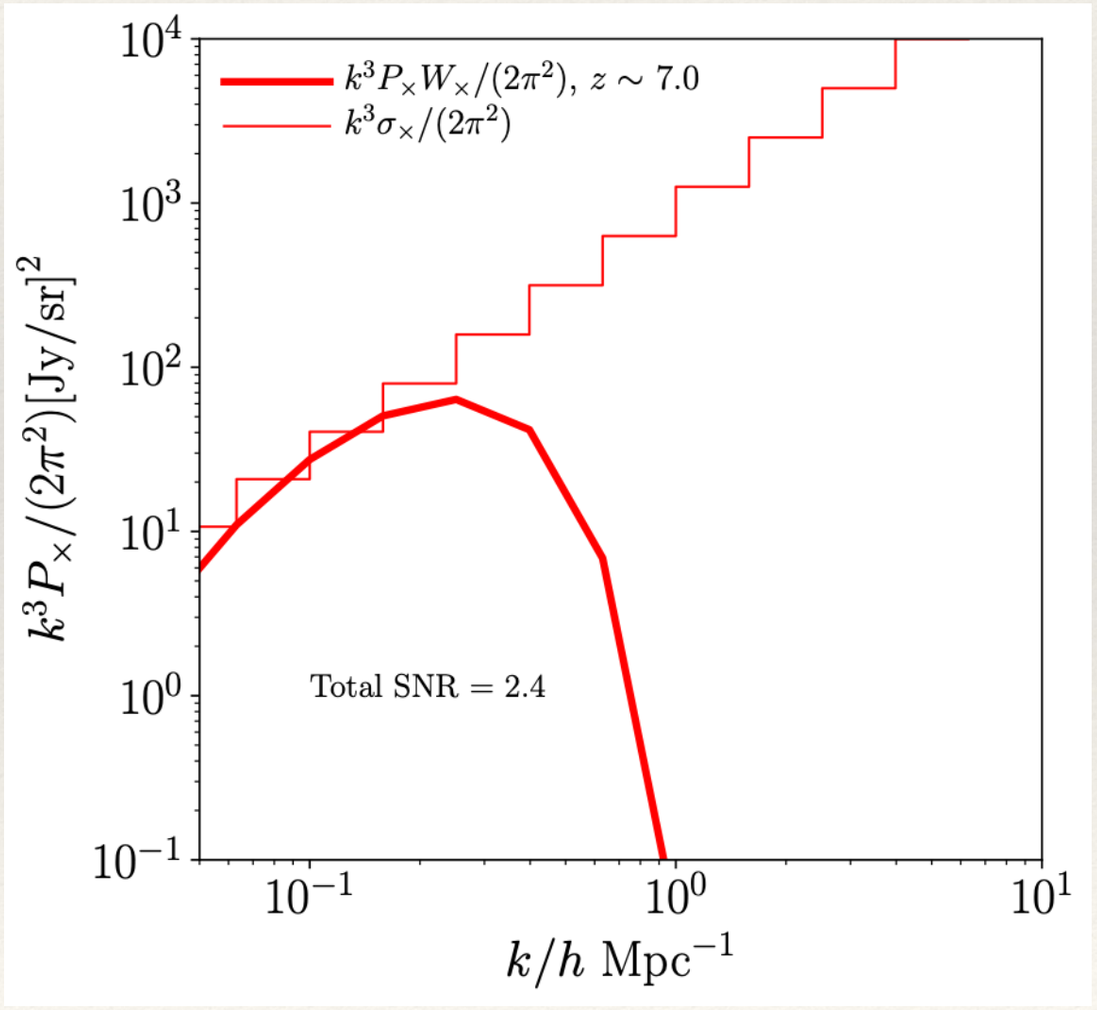

[HP (MNRAS, 2018), HP (MNRAS 2019), HP+ (MNRAS 2022), HP (MNRAS 2023, arXiv:2212.08077)]

To summarize …

Summary

- Line Intensity Mapping (IM): large volumes over a wide range of redshifts, species
- *Astrophysical systematic* in IM can be efficiently handled via a *data driven halo model, enabling …* **[HP+ (2015, 2016, 2017a, b), HP & Kulkarni (2017)]**
- …extensions to redshift space power spectra **[White (2001), Seljak (2000, 2001), HP (2021)]**
- Latest data from MeerKAT auto-correlation: characterization of the small scale structure of the HI intensity power spectrum
- Large-scale HI-halo mass relation consistent with halo model predictions, recent galaxy surveys **[Paul+ (2023), Bera+ (2022)]**
- Small-scales consistent for z ~ 0.32, may be evidence for higher than expected bias at z ~ 0.44; different possible causes; standard shot noise term favoured over FoG corrected version
- Sub-mm IM: several advantages, reduce systematics and foregrounds for 21 cm
- Improved versions of current architecture (EXCLAIM, FYST) reach secure to ***several 10 sigma detections*** in cross-correlation with MWA and SKA-LOW at $z \sim 5$-7

Thank you!

Redshift space: dark matter

[White (2000), Seljak (2000), Cooray and Sheth (2002) …]

$$P_{2\mathrm{h}}(k) = P_{\mathrm{lin}}(k)\left[\frac{1}{\bar{\rho}_{\mathrm{m}}}\int dM\, n(M) M b_{\mathrm{h}}(M)\left|u_{\mathrm{h}}(k\,|\,M)\right|\right]^2$$

Halo profile FT

$$P_{1\mathrm{h}}(k) = \frac{1}{\bar{\rho}_{\mathrm{m}}^2}\int dM n(M) M^2\,|\,u_{\mathrm{h}}(k\,|\,M)\,|^2$$

In redshift space $\quad \delta_{\mathrm{redshift}} = \delta_{\mathrm{real}}\left(1+f\mu^2\right)e^{-(k\sigma\mu)^2/2}$

$$\bar{P}^s_{2h}(k) = \left(1+\frac{2}{3}f+\frac{1}{5}f^2\right)P_{\mathrm{lin}}(k)\times\left[\int\frac{1}{\bar{\rho}_{\mathrm{m}}}\int dM\, n(M) M b_{\mathrm{h}}(M)\mathscr{R}_1(k\sigma)\left|u_{\mathrm{h}}(k;M)\right|\right]^2$$

$$\bar{P}^s_{1h}(k) = \frac{1}{(\bar{\rho}_m)^2}\int dM n(M) M^2\ \mathscr{R}_2(k\sigma)\,|\,u_{\mathrm{h}}(k;M)\,|^2$$

$$\mathscr{R}_1(y=k\sigma) = \sqrt{\frac{\pi}{2}}\frac{\mathrm{erf}(y/\sqrt{2})}{y}$$

$$\mathscr{R}_2(y=k\sigma) = \frac{\sqrt{\pi}}{8}\frac{\mathrm{erf}(y)}{y^5}\left[3f^2+4fy^2+4y^4\right]-\frac{e^{-y^2}}{4y^4}\left[f^2(3+2y^2)+4fy^2\right]$$

Redshift space: number weighted biased tracers (galaxies)

[Seljak (2000)]

$$P_{\rm g}^{2h}(k) = P_{\rm lin}(k)\left[\frac{1}{\bar{n}_g}\int dM\ M\ n(M)\langle N\rangle\ b_{\rm h}(M)u_g[k,M]\right]^2$$

Mean number density of galaxies

$$P_{\rm g}^{1h}(k) = \frac{1}{\bar{n}_g^2}\int dM\ n(M)\ \langle N(N-1)\rangle\,|\,u_g(k,M)\,|^2 + {\rm SN},$$

$$\delta^g_{\rm redshift} = \left(\delta^g_{\rm real} + \delta_{\rm h} f\mu^2\right), \delta_g \to \delta_g e^{-(k\sigma\mu)^2/2}$$

$$\bar{P}^s_g(k) = \left(F_{\rm g}^2 + \frac{2}{3}F_{\rm m}F_{\rm g} + \frac{1}{5}F_{\rm m}^2\right)P_{\rm lin}(k) + \frac{1}{\bar{n}_g^2}\int dM\ n(M)\ \langle N(N-1)\rangle\mathscr{R}_2(k\sigma)\,|\,u_{\rm g}(k,M)\,|^2$$

$$F_{\rm m} = \frac{f}{\bar{\rho}_{\rm m}}\int dM\ M\, n(M) b_{\rm h}(M)\,\mathscr{R}_1(k\sigma)u_{\rm h}(k,M),$$

$$F_{\rm g} = \frac{1}{\bar{n}_g}\int dM\ M\ n(M)\langle N\rangle b_{\rm h}(M)\mathscr{R}_1(k\sigma)u_{\rm g}(k,M)$$

Mean number of galaxies within a halo

Redshift space: mass weighted biased tracers (HI)

[HP (2021), HP+ (2023)]

Subtlety:
Shot noise with and without FoG term:

$$P_{\rm SN} = \frac{1}{\bar{\rho}^2_{\rm HI}} \int dM\, n(M) M^2_{\rm HI}$$

$$P^{\rm fog}_{\rm SN}(k) = \frac{1}{\bar{\rho}^2_{\rm HI}} \int dM\, n(M) M^2_{\rm HI}\, \mathscr{R}_3(k\sigma)$$

$$\mathscr{R}_3(y) = \frac{\sqrt{\pi}}{2} \frac{{\rm erf}(y)}{y} \,.$$